Response to interactive comment on *"Concentrations and radiative forcing of anthropogenic aerosols from 1750-2014 simulated with the OsloCTM3 and CEDS emission inventory"* by Marianne T. Lund, Gunnar Myhre, Amund S. Haslerud, Ragnhild B. Skeie, Jan Griesfeller, Stephen M. Platt, Rajesh Kumar, Cathrine Lund Myhre, Michael Schulz

Thank you for making us aware of the missing code availability section. We have added the information on how to access the code.

Response to review of *"Concentrations and radiative forcing of anthropogenic aerosols from 1750-2014 simulated with the OsloCTM3 and CEDS emission inventory"* by Marianne T. Lund, Gunnar Myhre, Amund S. Haslerud, Ragnhild B. Skeie, Jan Griesfeller, Stephen M. Platt, Rajesh Kumar, Cathrine Lund Myhre, Michael Schulz

We thank the anonymous referee for the careful and thorough review of our paper, and the useful suggestions. Responses to individual comments are given below.

Anonymous Referee #1
Received and published: 30 August 2018

General comments:
This paper evaluates the present-day aerosol distributions and radiative forcing in the latest OsloCTM3 chemical transport model. Surface concentrations, vertical distributions as well as aerosol optical depth are evaluated for the year 2010 against an extensive set of ground-based and satellite measurements. Uncertainties in the aerosol distributions are also assessed through a number of sensitivity studies assessing the uncertainty in the aerosol emissions, removal processes, meteorology and model resolution. The model is then used to assess the historical aerosol direct radiative forcing (RF) from 1750-2010. The net radiative forcing as well as the RF due to individual species are compared against the most recent published literature and CMIP5 estimates. Aerosol-cloud interactions are not assessed in this study.

This is a well-written, clearly presented, model evaluation manuscript. This paper does not document the latest updates to the OsloCTM3 model, but appropriate references are provided for this. Instead it documents the latest aerosol simulations with this model using the latest CMIP6 emissions inventory and subsequently derives the latest direct aerosol RF estimate. So I believe it is within the GMD scope as a Model Evaluation paper. This paper is timely given the CMIP6 project is now well underway and will provide a useful update to direct aerosol RF estimates in this regard. I recommend this paper to be published subject to a number of revisions I detail below.

Specific comments:
I struggled to appreciate the motivation for the additional sensitivity simulations conducted in this study. While these studies are useful and worth reporting the motivation for conducting these studies and link with the rest of the paper needs to be made clearer. This is probably most easily achieved in the Introduction.
Parts of the introduction has been rewritten in order to address this in a better and more explicit way. In particular, the following paragraph has been added:

"As accurate representation of the observed aerosol distributions in global models is crucial for confidence in estimates of radiative forcing (RF), these issues emphasize the need for broad and up-to-date evaluation of model performance.
The diversity of simulated aerosol distributions, and discrepancies between models and measurements, stem from uncertainties in the model representation aerosol processing. Knowledge of the factors that control the atmospheric distributions is therefore needed to identify potential model improvements and need for further observational data, and to assess how remaining uncertainties affect the modeled aerosol abundances and, in turn, estimates of RF and climate impact. A number of recent studies have investigated the impact of changes in aging and scavenging processes on BC distribution, focusing on aging and wet scavenging processes (e.g., [Bourgeois and Bey, 2011; Browse et al., 2012; Fan et al.,

2012; Hodnebrog et al., 2014; Kipling et al., 2013; Lund et al., 2017; Mahmood et al., 2016]), resulting in notable improvements, at least for specific regions or observational data sets. However, with some notable exceptions (e.g., [e.g., Kipling et al., 2016]), fewer studies have focused on impacts of scavenging and other processes on a broader set of aerosol species or the combined impact in terms of total aerosol optical depth (AOD)."

In Sect 2.3 Please report the length of each time slice simulation and how this impacts the signal to noise in resulting RF estimates. Are you running 20-30 years for each time slice?
Each simulation is one year, with six months spin up. Text has been clarified and now reads:
"All simulations are one year with six months spin-up. "

In Sect 3.3 please describe clearly either explicitly or through appropriate references how you calculated the RFari. Have you calculated an effective radiative forcing or used the more traditional radiative forcing metric? It is currently unclear. Also, how are the individual species RFari determined - through species only runs or is the RT code able to output this?. Please provide this detail in the manuscript.
Regarding the first half of this comment: The radiative forcing calculations described in detail in Sect. 2.4 of the paper, including a definition of RFari, i.e., forcing due to aerosol-radiation interactions, not including any rapid adjustments as for the effective RF. To clarify, we refer to back to the description in Sect. 3.3. The species-specific RFari is obtained by individual runs, where the concentration of the respective species is set to the pre-industrial level. This has been clarified in the text:
"The RFari of individual aerosols is obtained by separate simulations, where the concentration of the respective species is set to the pre-industrial level."

Use of older version of CEDS emission inventory: I am not convinced that the historical RFari will not be impacted at all by the choice of CEDS emission inventory. Changes in spatial distribution of emission could impact aerosol removal, transport and thus lifetime, temporal shifts in the distribution could also potentially impact the historical evolution of the ERF. While I understand the computational burden of repeating all tests, two runs using the new CEDS version with 1750 and for instance year 2010 emissions would allow you to quantify the impact on the RF fairly easily to allow you to justify it in the text. It looks like you may have the 2010 simulation already from you Fig S4 plots.
We have repeated the 1750 simulation with the new CEDS version 2017 inventory and calculate a 2% stronger net RFari (2010 relative to 1750) than with the 2016 version. Global burdens differ by 2-10% between runs with the two inventories, showing that there is some impact through removal and transport. The impact on net RFari is a combination of a slightly higher BC burden and lower sulfate and OA burden. Here limit the analysis to direct aerosol effects only. RFari scales more with the total burden changes, which are small. As the reviewer points out, the effect of spatial changes in the aerosol distribution could be more important for the ERF, i.e., also considering aerosol-cloud interactions.

Furthermore limiting your evaluation to BC is also questionable as I would expect notable differences in for instance SO2. I would request that you extend this evaluation over the USA to all aerosol species where you have observations.
We agree and have extended the comparison to organic aerosol, nitrate and sulfate, as well measurements over in Asia and Europe. Figure S4 has been updated and the following text is added:
"While repeating all simulations require more resources than available, we have performed an additional run for the year 2010. Figure S4 shows the comparison of modeled concentrations against IMPROVE measurements with the two emission inventory versions, CEDSv16 and CEDSv17. In the case of BC, the comparison shows a 5% higher correlation and 15% lower RMSE with the CEDSv17 than CEDSv16. A similar improvement is found for nitrate, with 26% higher correlation and 12% lower RMSE, while in the case of OC and sulfate, the difference is small (< 5%). Smaller differences of between 2-10% are also found

in the comparison against measurements in Europe and Asia (not shown). Hence, using the updated version of the emission inventory has an effect on the model performance in terms of surface concentrations, but without changing the overall features or conclusions. The net RFari in 2010 relative to 1750 is 2% stronger with the CEDSv17 inventory, a combined effect of slightly higher global BC burden and lower burdens of sulfate and OA.”

Changes to the large-scale ice scavenging efficiency have a large control on the global aerosol distribution. The paper would benefit from a more detailed description of how the LS ice (and liquid) scavenging is parameterized in the model in Sect 2.1
The paragraph on removal has been expanded with more details and now reads:

“Aerosol removal includes dry deposition and washout by convective and large-scale rain. Rainfall is calculated based on European Center for Medium-Range Weather Forecast (ECMWF) data for convective activity, cloud fraction and rain fall. The efficiency with which aerosols are scavenged by the precipitation in a grid box is determined by a fixed fraction representing the fraction of this box that is available for removal, while the rest is assumed to be hydrophobic. The parameterization distinguishes between large-scale precipitation in the ice and liquid phase, and the OsloCTM3 has a more complex cloud model than OsloCTM2 that accounts for overlapping clouds and rain based on [Neu and Prather, 2012]. When rain containing species falls into a grid box with drier air it will experience reversible evaporation. Ice scavenging, on the other hand, can be either reversible or irreversible. For further details about large-scale removal we refer the reader to Neu and Prather [2012]. Convective scavenging is based on the Tiedtke mass flux scheme (Tiedtke 1989) and is unchanged from the OsloCTM2. The solubility of aerosols is given by constant fractions, given for each species and type of precipitation (i.e., large-scale rain, large-scale ice, and convective) (Table 2). Dry deposition rates are unchanged from OsloCTM2, but the OsloCTM3 includes a more detailed land use dataset (18 land surface categories at 1°x1° horizontal resolution compared to 5 categories at T42 resolution), which affects the weighting of deposition rates for different vegetation categories. Re-suspension of dry deposited aerosols is not treated.”

Technical corrections:
Line 70: 2011 - this should be 2010
IPCC AR5 give the forcing in 2011 relative to 1750. However, we see that there is a typo in our abstract, where 2010 is used. This has been corrected.

Line 170: It would be worthwhile to report here what global scaling factor you have used in the Gantt parametersation of marine OM. Gantt et al. 2015 I think use a global scaling factor of 6 but this is believed to be highly model dependent.
This is good point. Using the scaling factor of 6 from Gantt et al. produces too high emissions in our model. The scaling factor is also dependent on the sea salt production scheme and, to some degree, on resolution. With the sea salt scheme used here, we use a factor of 0.5. The text has been updated and reads:

“The scaling factor depends on the chosen sea salt production scheme (see below) and to some degree on the resolution; here we have used a factor of 0.5. “

Line 281: Explicity state the aerosol concentration threshold below which you apply the Bond and Bergstrom method. Why do you change approaches? Again state the motivation for these different approaches in different regimes and why they need to be made. Does Zanatta lead to too high a MAC in

the low aerosol regimes? Has this been constrained by observations - if yes, provide appropriate reference here. Some discussion of the uncertainties in both approaches as this links to your uncertainties in BC RFari discussed in Sect 3.3

We have included the following description in the manuscript:

"The measurements in Zanatta et al. [2016] represent continental European levels. For very low concentrations of BC, the formula given in Zanatta et al. [2016] provides very high MAC values. We have therefore set a minimum level of BC of 1.0e-10 g m^{-3} for using this parameterization, and for lower concentrations we use [Bond and Bergstrom, 2006]. In addition, we have set a maximum value of MAC of 15 m^2 g^{-1} (637 nm) to avoid unrealistic high values of MAC compared to observed values."

Line 329-330: It would be useful here to be clear on what model variables you've sampled at 3 hour resolution and what ones you've sampled monthly and why you needed to do this.

Text has been clarified:

"the model data is linearly interpolated to the location of each station using annual mean, monthly mean (concentrations) or 3-hourly output (AOD), depending on the resolution of the observations."

Line 452: EBAS - I think this should refer to EMEP/ACTRIS. EBAS has not been previously mentioned.

Yes, thank you for pointing this out.

Line 468: Remove "as for surface concentrations,"

Removed.

Table 3: It would be useful to have the % change in burden listed alongside the burdens of all the sensitivity experiments. Perhaps in parentheses next to the burdens.

We tried this, but we think that it exacerbated the readability of the table without adding much useful information as these numbers are easily calculated from the absolute values. We have therefore chosen to leave this table as is.

Line 541-544: Can you actually make this statement? You do not show any impact on surface concentrations. I do not think this paragraph adds any value to the manuscript and would remove.

The evaluation against surface concentration measurements does suggest an improvement in model performance with the newer emission inventories, but similar performance in the other sensitivity tests. However, as this is first covered in the following section, we see that this paragraph seems a bit out of context here and we have removed it.

Line 555: Could the higher correlation and lower bias found in the 1x1RES test not just be a consequence of improved spatial sampling in your comparison and not actually due to an improved distribution of AOD? As you do not evaluate the species whose emissions would depend more strongly on resolution (ie: dust, sea salt) it's hard to quantify the benefit here.

This is a good point, and based on previous studies of the impact of sampling and the coarseness of typical model horizontal grids on comparisons with (in particular AOD), we would expect an improved sampling to play a role here. This point is now made in the manuscript:

"For both observables, the improvement in the 1x1RES simulation may result from a better sampling at a finer resolution, improved spatial distribution or a combination. "

Line 638: OsloCTM3fast - what is this?? There is no prior mention of a fast configuration!!

Thanks for pointing this out, it is an error and has been corrected.

Line 688: "These results emphasize the importance of assumptions related to the BC absorption" –> these results emphasize the importance of assumptions and uncertainties related to the BC absorption.

Corrected.

Figure 6: It would be more informative to show obs +/- 1 standard deviation instead of just + 1 std.
After trying different versions, we have rather added the 25/75 percentiles as a shading to show spread in both directions.

Table S2: Column 2 you use MNB instead of NMB
Corrected, this is a typo and should be NMB here as well.

Response to review of *"Concentrations and radiative forcing of anthropogenic aerosols from 1750-2014 simulated with the OsloCTM3 and CEDS emission inventory"* by Marianne T. Lund, Gunnar Myhre, Amund S. Haslerud, Ragnhild B. Skeie, Jan Griesfeller, Stephen M. Platt, Rajesh Kumar, Cathrine Lund Myhre, Michael Schulz

We thank the anonymous referee for the careful and thorough review of our paper, and the useful suggestions. Responses to individual comments are given below.

Anonymous Referee #2
Received and published: 18 September 2018

In this paper, the authors describe updates made to aerosol representations in the Oslo Chemistry Transport Model, compare the simulated aerosol to various observations, and use that model with a recent emission dataset to derive the time series of radiative forcing of aerosol-radiation interactions (RFari) over the industrial era. Their estimate of RFari is at the weaker end of latest AeroCom and IPCC assessments, and the authors work suggest that globally-averaged RFari has weakened since the 1980s. The paper is nicely written and to the point. Figures are well chosen and illustrate the discussion well. Sensitivity studies are interesting. There are a few aspects that can be clarified however: The justification for model parameters is often lacking and there is also a need to better link section 3.3 on RFari timeseries with model evaluation. Below I list the clarifications that I would like to see ahead of the paper's publication. Addressing those comments should not require additional analysis, so represent minor revisions.

1 Comments
• Abstract, line 38: Be more specific about what is new about the treatment of black carbon in OsloCTM3
Clarified. The text now reads:
"The treatment of black carbon (BC) scavenging in OsloCTM3"

• Abstract, line 47: Aren't the AR5 forcing estimates for 2011?
Yes, this is a typo, thanks for noticing.

• Introduction, line 76: Are those the CMIP5 historical emissions documented by Lamarque et al., doi:10.5194/acp-10-7017-2010, 2010? If so, then reference the paper here.
Yes, reference included.

• Introduction, line 77: I seem to remember that historical finished in 2005, not 2000, in CMIP5.
Corrected. In fact, this sentence confused the inventory documented by Lamarque (1850-2000) with the CMIP5 experimental design with historical period 1850-2005. For clarification, we have rephrased slightly, adding referring to both Lamarque et al. 2010 and Taylor et al. 2012. The paragraph now reads:

"The Community Emissions Data System (CEDS) recently published a new time series of emissions from 1750 to 2014, which will be used in the upcoming CMIP6 [Hoesly et al., 2018]. CEDS includes several improvements, including annual temporal resolution with seasonal cycles, consistent methodology between different species, and extending the time series to more recent years, compared to previous inventories and assessments [e.g., Lamarque et al., 2010; Taylor et al., 2012]."

• Introduction, lines 114–116: Is that sentence still talking about scavenging?

Scavenging and other processes. Text clarified:
"(…) few studies have focused on impacts of scavenging and other processes on a broader set of aerosol species or the combined impact in terms of total aerosol optical depth (AOD)."

• Section 2.1, line 157: What are the finer spatial and temporal resolutions of the new transfer rates?
Monthly instead of seasonal and latitudinal rates established based on simulations of 10 instead of four emission source regions, covering not only the northern hemisphere, but giving near global coverage. Now specified in the text:
"Specifically, the latitudinal transfer rates have been established based on experiments with 10 instead of four emission source regions and with monthly, not seasonal resolution."

• Section 2.1, lines 161–163, line 203, and Table 2; and Section 2.4, lines 284–285: The numbers selected for OC-OM conversion, hydrophilic fractions of BC and OM, aerosol solubility fractions, and absorbing OM fractions need to be justified. Where do they come from?
References to OC-OM conversion and hydrophilic fractions of BC and OM added.

On the OM fraction we have added the following:
"*Organic matter has a large variation in the degree of absorption [e.g., Kirchstetter et al., 2004; Xie et al., 2017], from almost no absorption to a strong absorption in the ultraviolet region. Here, we have implemented absorbing organic matter according to refractive indices from Kirchstetter et al. [2004]. The degree of absorption varies by source and region and is at present inadequate quantified: Here we assume 1/3 of the biofuel organic matter and ½ of the SOA from anthropogenic volatile organic carbon (VOC) precursors. The remaining fractions of biofuel, fossil fuel and marine POA and SOA (anthropogenic and all natural VOCs) are assumed to be purely scattering organic matter. As these fractions are not sufficiently constrained by observational data and associated with significant uncertainty, we also perform calculations with no absorption by OA."*

• Section 2.1, lines 169–170: How is the scaling of marine OM emissions done in practice? Sea spray is dependent on wind speed, so do you need to run the model a first time to get OM emissions, then scale them, then run again?
The scaling is done by multiplying with a fixed factor, determined from previous test runs, which depends on the sea salt production scheme used (here the factor is 0.5). The exact scaling depends on meteorology and resolution, found to result in inaccuracies of 3-5%. The marine OM emissions is checked after the run to make sure that no additional tuning of the scaling factor is needed beyond these uncertainties. We have specified the scaling factor in the text based on comments by both referees. The following has been added:
"The scaling factor depends on the chosen sea salt production scheme (see below) and to some degree on the resolution; here we have used a factor of 0.5. "

• Section 2.1, line 195: Why does the DEAD scheme need energy budget calculations?
Radiative fluxes are needed for calculation of boundary layer properties related to the dust mobilization. For clarification we have added:
"As a minor update, radiative flux calculations, required for determination of boundary layer properties in the dust mobilization parameterization [Zender et al., 2003], now uses radiative surface properties and soil moisture from the meteorological fields."

• Section 2.1, paragraph starting line 198: Does the model account for reevaporation of precipitation? And re-suspension of dry-deposited aerosol?

The model treats evaporation (reversible and irreversible), but not re-suspension. Following this comment, and comment from anonymous referee #1, we have expanded the description of removal in Sect. 2.1, including these specifications.

• Section 2.3, line 249: Why fix the meteorology to 2010? Once reanalysis data is available (from 1979 for ERA, I believe), then it would be good to use the meteorology that corresponds to the actual year. There is a sensitivity study dedicated to the impact of meteorology, and that impact is fairly sizeable (lines 556–558). So using 2010 for all years does not seem ideal.

Because re-analysis data is only available for a limited period of the historical time series considered here, we maintain that keeping meteorological data constant is a reasonable experimental design for a study with our objective, for consistency and in order to isolate the effect of change in the emissions. Moreover, RF is calculated relative to pre-industrial, where we have no way of using "real" meteorological data. As recent study by Myhre et al. 2017 looked at the effect of emission changes over the 1990-2014 period, and in this case meteorology for each year was used in some of the models.

Our sensitivity test gives an indication of the order of magnitude impact on the aerosol burden and, as the direct RF scales quite linearly with aerosol burden, on the consequent RF. Using the rather extreme case of opposite ENSO phases, we find burden changes of 1-10%, suggesting that using constant meteorological input data is unlikely to change conclusions about the overall trends

Use of correct meteorological data is of course important for accurate distribution of concentrations and model evaluation, which is why we limit our validation to the year 2010.

• Section 2.3, paragraph starting line 254: It would be good to have more insight into the choice of sensitivity studies of removal. Why no SOLINC sensitivity study, for example?

The following text has been added for clarification:

"To modify the scavenging, we tune the fixed fractions that control aerosol removal efficiency in the model (see Sect. 2.1). Table 2 summarizes fractions used in the baseline configuration and the three sensitivity tests. A decrease and increase in efficiency of 0.2 is adopted for scavenging of all aerosols by liquid clouds (except hydrophobic BC and OM) and ice clouds, respectively. Note that there is no test with increased removal by liquid clouds, as, with the exception of hydrophobic BC, OM and SOA, 100% efficiency is already assumed. For ice clouds, we also reduce the efficiency to a fraction of 0.1, or 0.001 if the value is 0.1 in the baseline configuration. We note that these changes do not represent realistic uncertainty ranges based on experimental or observational evidence, as there are limited constraints in the literature, but are chosen to explore the impact of a spread in the efficiency with which aerosols act as ice and cloud condensation nuclei."

• Section 2.3, line 258: I do not think that the resolution of the control simulation has been given at this stage, but I may have missed it.

The resolution is given in the paragraph before.

• Section 2.4, paragraph starting line 270: It would be useful to have a Table summarizing the assumptions made about size distribution and refractive index (or MEC/MAC if that is what the model uses) for all modelled species, with references where appropriate. That information is crucial to understanding differences in radiative forcing efficiencies between models, yet is rarely given in model description papers.

We believe that this information is readily enough available from the references (Myhre et al. 2007, Myhre et al. 2009) in Sect. 2.4, with updates subsequently described.A table with this information has been included in the supplementary material. However, we have added a table in the supplementary material with changes in burden, AOD, AAOD, RFari, and normalized RF over the period 1750-2010 given for individual aerosol components, as well as the net RFari. This information has been commonly presented in previous studies and will allow the reader to better understand differences compared to the present analysis. The text has been updated accordingly.

• Section 2.5, line 297: "frameworks" – did you mean networks?

Yes, error corrected.

• Section 2.5, lines 321–322: What does the AeroCom validation tool do?

Probably poor/unclear chose of wording: The comparison between the model and measurement is done through the AeroCom data base, i.e., model data is interpolated and extracted for each location of the AERONET stations (this method is already described in a later paragraph). We have clarified the sentence:

"The comparison with AERONET data was done using processed through the validation tools available from the AeroCom data base hosted by Met Norway."

• Section 3.1 starting line 354: It would be most useful to also include residence times for each species in Table 3. Perhaps in parentheses after the burden? Residence times are also crucial to understanding differences in aerosol distributions among models.

Good suggestion, we agree that this is useful additional information. We have included the residence times for the baseline simulation in Table 3, with remaining simulations in a separate table in the supplementary material (for readability).

• Section 3.1, paragraph starting line 356: The authors try to explain differences with the previous version of the model, which is great, but that is not done consistently. Why is sulfate burden 35% higher than in OsloCTM2? (Line 360.) Is that understood? And what explains the 25% higher OA burden? According to lines 369–370, the marine POA contribution is too small to explain that large difference.

We have added the following for sulfate:

"While the total SO_2 emission is only 5% higher in the present study than in the OsloCTM2 AeroCom III simulation, the atmospheric residence time of sulfate is 50% longer, suggesting that the burden difference is mainly attributable to changes in the parameterization of dry and large-scale wet deposition (Sect. 2.1)."

And modified the OA discussion:

"The OsloCTM3 estimate includes the contribution from marine OA emissions (Sect. 2.1), which may explain part of the difference as marine OA was included in some of the AeroCom II models, but not OsloCTM2. Additionally, the residence time of OA of 5.3 days is longer than in the OsloCTM2 AeroCom II experiment."

• Section 3.1, line 377: "against output" – it is the other way around, model versus observations.

The sentence is technically correct as it stands, I think, but I can see that it would be more as expected to start with the model output and have switched it around for clarification:

"Figure 1 shows results from the baseline OsloCTM3 simulation against annual mean measured surface concentrations of EC, OC, sulfate and nitrate in Europe, North America and Asia."

• Section 3.1, line 384: What correlation? Need to rephrase to clarify that sentence.

With CAWNET observations. Rephrased for clarification:

"In contrast, the correlation with CAWNET observations is generally similar to, or higher than, other regions/networks."

• Section 3.1, line 414: Is being close to the AeroCom nitrate multi-model mean a good thing? How do models compare to observations in Bian et al. 2017?

Good point. We have added the following:

"Results showed that most models tend to underestimate ammonium concentrations compared to observations in North America, Europe and East Asia, with a multi-model mean bias and correlation of

0.886 and 0.47, respectively. Tthe OsloCTM3 shows good agreement with ammonium measurements in North America, but has a bias and correlation close the model average in the other two regions. "

• Section 3.1, lines 426–428: Erroneous emissions have a big impact on model performance. Can't you re-run at all? That would be a shame.
We did re-run the year 2010 simulation for the assessment of impact described in this paragraph. In the revised manuscript, the documentation of the impact of the updated CEDS emissions on model performance is also extended to more species and the following text has been added:
"While repeating all simulations require more resources than available, we have performed an additional run for the year 2010. Figure S4 shows the comparison of modeled concentrations against IMPROVE measurements with the two emission inventory versions, CEDSv16 and CEDSv17. In the case of BC, the comparison shows a 5% higher correlation and 15% lower RMSE with the CEDSv17 than CEDSv16. A similar improvement is found for nitrate, with 26% higher correlation and 12% lower RMSE, while in the case of OC and sulfate, the difference is small (< 5%). Smaller differences of between 2-10% are also found in the comparison against measurements in Europe and Asia (not shown). Hence, using the updated version of the emission inventory has an effect on the model performance in terms of surface concentrations, but without changing the overall features or conclusions."

As global and national emission totals are unchanged between the two inventory versions, and we consider only the direct radiative effect, we believe that the implications for the RF estimates is small. We confirm this by also repeating the 1750 simulation as part of the revision: the RFari (2010-1750) is 2% stronger with the CEDSv17 inventory.

• Section 3.1, Figure 2: Could you show numbers in each slice of the pie chart in Figure 2? That would help make the comparison more quantitative.
Yes, done.

• Section 3.1, paragraph starting line 453: Figure 3d suggests that the model overestimates low optical depths but underestimates large optical depths. Is that correct? From experience, it is a common model deficiency, It may have even been noted in an AeroCom paper.
Yes, the model overestimates the very lowest measured AOD values. The most pronounced underestimation is seen for AOD around 0.1 to 1.0, but with a tendency towards more underestimation than overestimation also for the highest measured values. However, we are not aware of any AeroCom papers or multi-model studies documenting similar results that we could base a discussion around.

• Section 3.1, line 468: Small addition for clarity: "there are notable difference in model performance"
Included.

• Section 3.2, line 502: The analysis should point to Table 2 to make sense of sensitivities to wet removal. Species with the same scavenging fractions are likely to behave similarly in such sensitivity studies.
Good point. Included.

• Section 3.2, lines 519–520 and Figure 4: What is happening in North America? The change is in the Midwest, whereas I would have put the source regions more to the East.
Upon closer inspection of the burden of individual components, we see that this increase in total AOD in Central North America is mainly driven by an increase in ammonium nitrate. There is actually a dipole pattern in the ammonium nitrate change with different emission inventories: a lower burden is found in the Easternmost US (i.e., east of approx. 90W) and a notable increase in burden in the Midwest when ECLv5 and CMIP5 emissions are used. The former is likely due to the higher SO2 emissions in these inventories than in CMIP6, which is mainly confined to the east and south along the Mexican Gulf. The increased burden likely results from the increase in NOx emissions, which extends into the states of

Kansas, Oklahoma and Nebraska, and beyond. At the same time there is slight decrease in SO2 emissions in the western part of the US, which reduces sulfate concentration and hence competition for available ammonia. In the ECLv5 inventory, there are also higher emissions of NH3. We have added the following to the discussion:

"Over central North America the AOD is higher, mainly due to more ammonium nitrate, whereas the higher AOD over Eastern Europe and part of Russia is a result on higher sulfate concentrations."

• Section 3.2, lines 526–527 and Figure 4: What is happening with dust in METDTA? Also a teleconnection with ENSO?
Presumably, this refers to the ratio of total AOD in figure 4 and the area with values above one off the coast of North Africa, where the dust influence on AOD is prominent. The influence of met-data on dust occur through both production and transport/scavenging. There are some studies suggesting impacts of ENSO on precipitation in Sahel, and given that we have selected years of opposite ENSO phase, it is likely that we see an impact. However, other meteorological differences will also play a role and cannot be distinguished. While we cannot provide a quantitative answer, we have added the following to the discussion:

"There is also a notable change in the Atlantic Ocean, where mineral dust is a dominating species. The meteorological data can affect production, deposition and transport of dust directly, as well as indirectly through ENSO-induced teleconnections as suggested by e.g., Parhi et al. [2016]."

• Section 3.2, lines 530–531: Why such a strong dependence of nitrate on emission inventory? The vertical profile of ammonium nitrate formation is determined by temperature and competition from ammonium sulfate, so the role of emission inventories is not obvious. Which emission differences matter: ammonia or sulfur dioxide?
The change in nitrate formation is a complex interplay of changes in several gases (SO2, NH3 and NOx) and the differences in these, in turn, vary between inventory, as well as region. Hence, a significant impact of emission inventory is not unexpected. However, it is interesting to note the stronger effect on emissions, and less impact of changes to the scavenging, on the burden of nitrate, and the contrast to the other species. Based on this comment and the one above, we have added the following:

"In general, the burden of BC, OA and dust is significantly affected by changes in the scavenging assumptions, while nitrate responds more strongly to different emission inventories, likely due to the complicated dependence on emissions of several precursors and competition with ammonium-sulfate. We also note that at higher altitudes the absolute differences in the burden of nitrate are small."

With the data available from the simulations in the present study, we cannot quantify the roles of the respective emission difference. There are also likely strong seasonal and geographical variations. However, an inspection of the spatial distribution of differences in emissions, zonal mean concentrations and burden, can shed some light on the driver. It also important to point out that at high altitudes, nitrate values are small, as are the absolute differences.

For RCP/CMIP5 emissions, the global mean vertical profile of nitrate is lower than then using CMIP6 emissions throughout the atmosphere, mainly determined by a decrease in concentration between 10 and 40N. Compared to the CMIP6 inventory, RCP/CMIP5 emissions of both NH3 are lower in Asia, North Africa and South America. NOx is also lower, in particular in Asia. (SO2 emissions in India are somewhat lower as well, but we do not know to what extent less completion for available ammonia offsets an overall lower amount of precursors.) NOx is also lower in South Asia in ECLv5, while sulfate is higher, the combined effect being a lower nitrate burden. However, for nitrate there is a higher concentration around 15-40S and 35-50N, especially 800 and 400 hPa. This seems to arise, at least in part, from higher NH3 emissions, and areas with lower SO2, in China, South America and central Africa. So in summary, changes to all three gases seem to contribute, but with different roles in different regions.

• Section 3.2, lines 537–540: Again, should link to Table 2.
Done.

• Section 3.3 starting line 618: It would most interesting to link specific model deficiencies to errors in RFari estimates. This is done briefly in the discussion, but could be done more clearly in section 3.3. For example, he model generally underestimate surface concentrations. Does that bias cancel out when taking differences over the industrial era? Another example is that the model underestimates aerosol in Asia. Does that mean that recent RFari is underestimated? Or that similar underestimations would have happened over US/Europe when sulfate was high in those regions in the 1950-1980s? A final example is about high latitudes. There is a confident conclusion about RFari changes north of 70_N (lines 679–681), but do you really have confidence in your model in that region?
It is not straightforward to investigate indications of biases from comparisons to observations and the implication for RF. A bias compared to surface measurements may not necessarily imply that the total column has the same bias. Moreover, even if there is an underestimation of the total AOD, the influence of such a bias on RF depends on the mix of absorbing and scattering aerosol. Similarly, the aerosol mix is an important complicating factor the effect of underestimated or missing emission sources, for instance in Asia, where the uncertainties in the emissions are larger than in other regions. At high latitudes, the model does show an underestimation of BC concentrations, both at the surface and at higher altitudes. However, this is mainly an issue during winter and early spring, when the direct aerosol effect is small due to lack of sunlight. For other species and AOD, the availability of observations is a limiting factor. Additionally, we cannot perform a detailed evaluation of the simulated pre-industrial concentrations.

As the referee notes, the manuscript already discusses some of these issues. For the reasons noted above, we are reluctant to speculate too much beyond these more general points or attempt too specific links between model deficiencies and RF estimates. However, we have restructured Section 4 slightly, to make this discussion easier to follow and included a couple of additional issues. The paragraph now reads:

"A significant range from -0.6 to -0.13 W m-2 surrounds the central RFari estimate of -0.35 W m-2 from IPCC AR5 [Boucher et al., 2013], caused by the large spread in underlying simulated aerosol distributions. Deficiencies in the ability of global models to reproduce atmospheric aerosol concentrations can propagate to uncertainties in RF estimates. As shown in Sect. 3, the OsloCTM3 generally lies close to or above the multi-model mean of anthropogenic aerosol burdens from recent studies and is found to perform reasonably well compared with observations and other global models, with improvements over the predecessor OsloCTM2. In particular, recent progress towards constraining the vertical distribution of BC concentrations has resulted in improved agreement between modeled and observed vertical BC profiles over the Pacific Ocean with less of the high-altitude overestimation seen in earlier studies. However, as shown by Lund et al. [2018], there are discrepancies compared to recent aircraft measurements over the Atlantic Ocean. A remaining challenge is the model underestimation of Arctic BC concentrations. However, this is seen mainly during winter and early spring, when the direct aerosol effect is small due to lack of sunlight. In contrast, the higher emissions in the CEDSv16 inventory also results in an improved agreement with BC surface concentrations over Asia. In general, we find lower surface sulfate concentrations in the model compared with measurements. This could contribute to an underestimation of the sulfate RFari, which is weaker in the present study than in IPCC AR5. An underestimation of observed AOD in Asia is also found, however, the implication of this bias on RF is not straightforward to assess, as it is complicated by the mix of absorbing and scattering aerosols. (…)"

• Section 3.3, line 638: What is "OsloCTM3fast"?
This is a typo, there is no fast version of the model. Corrected.

• Section 3.3, line 675: "clearly" – Not that strong a signal really. Did the radiative forcing efficiency change with the change in emitting region? Combining by eye the two panels of Figure 8 would suggest that the change is rather small.

We think that the decline in net RFari north of 40°N is quite clearly seen in this figure, as is the strengthening between 10-30°N. However, the peak RFari is indeed significantly lower in 2014 than it was in 1970-90s. This is in large part due to the different evolution of scattering and absorbing aerosols, where sulfate burden is lower than in the late 20th century, while the BC burden has contributed to increase. There may also be an influence of different forcing efficiencies, however, since we only consider direct radiative effects, it is likely to be smaller than the impact of changing relative importance of scattering and absorbing aerosols. To clarify, we have modified the text:

"Over the past decades, there has been shift in emissions, from North America and Europe to South and East Asia. This is also reflected in the zonally averaged net RFari over time in Fig. 8b. RFari declined in magnitude north of 40°N after 1980, with particularly large year-to-year decreases between 1990 and 1995, and from 2005 to 2010, and strengthened in magnitude between 10°-30°N. The RFari also strengthened in the Southern Hemisphere subtropical region, reflecting incresing emission in Africa and South America after 1970. However, the peak net RFari is considerably weaker in 2014 than the peak in 1980. This mainly is due to fact that simultaneously with the southwards shift, the sulfate burden has declined, while the BC burden has increased steadily at the same latitudes, resulting in a weaker net forcing."

Concentrations and radiative forcing of anthropogenic aerosols from 1750-2014 simulated with the OsloCTM3 and CEDS emission inventory

Marianne Tronstad Lund[1*], Gunnar Myhre[1], Amund Søvde Haslerud[1], Ragnhild Bieltvedt Skeie[1], Jan Griesfeller[2], Stephen M. Platt[3], Rajesh Kumar[4,5], Cathrine Lund Myhre[3], Michael Schulz[2]

1 CICERO Center for International Climate Research, Oslo, Norway

2 Norwegian Meteorological Institute, Oslo, Norway

3 NILU – Norsk institutt for luftforskning, Dept. Atmospheric and Climate Research (ATMOS), Kjeller, Norway

4 Advanced Study Program, National Center for Atmospheric Research, Boulder, Colorado, USA

5 Atmospheric Chemistry Division, National Center for Atmospheric Research, Boulder, Colorado, USA

*Corresponding author: m.t.lund@cicero.oslo.no

Abstract

We document the ability of the new generation Oslo chemistry-transport model, OsloCTM3, to accurately simulate present-day aerosol distributions. The model is then used with the new Community Emission Data System (CEDS) historical emission inventory to provide updated time series of anthropogenic aerosol concentrations and consequent direct radiative forcing (RFari) from 1750 to 2014.

Overall, the OsloCTM3 performs well compared with measurements of surface concentrations and remotely sensed aerosol optical depth. Concentrations are underestimated in Asia, but the higher emissions in CEDS than previous inventories result in improvements compared to observations. The treatment of black carbon (BC) treatment scavenging in OsloCTM3 gives better agreement with observed vertical BC profiles relative to the predecessor OsloCTM2. However, Arctic wintertime BC concentrations remain underestimated, and a range of sensitivity tests indicate that better physical understanding of processes associated with atmospheric BC processing is required to simultaneously reproduce both the observed features. Uncertainties in model input data, resolution and scavenging affects the distribution of all aerosols species, especially at high latitudes and altitudes. However, we find no evidence of consistently better model performance across all observables and regions in the sensitivity tests than in the baseline configuration.

Using CEDS, we estimate a total net RFari in 2014 relative to 1750 of -0.17 W m^{-2}, significantly weaker than the IPCC AR5 2011̶0-1750 estimate. Differences are attributable to several factors, including stronger absorption by organic aerosol, updated parameterization of BC absorption, and reduced sulfate cooling. The trend towards a weaker RFari over recent years is more pronounced than in the IPCC AR5, illustrating the importance of capturing recent regional emission changes.

60

61

1 Introduction

63

Changes in anthropogenic emissions over the industrial period have significantly altered the abundance, composition and properties of atmospheric aerosols, causing a change in the radiative energy balance. The net energy balance change is determined by a complex interplay of different types of aerosols and their interactions with radiation and clouds, causing both positive (warming) and negative (cooling) radiative impacts. Global aerosols were estimated by the Intergovernmental Panel on Climate Change fifth assessment report (IPCC AR5) to have caused a~~n total~~n effective radiative forcing (ERF) of -0.9 W m^{-2} over the industrial era from 1750 to 2011, but with considerable uncertainty (-1.9 to -0.1 W m^{-2}) [*Boucher et al.*, 2013]. This large uncertainty range arises from a number of factors, including uncertainties in emissions and the simulated spatiotemporal distribution of aerosols, their chemical composition and properties.

~~This large uncertainty range arises from a number of factors, including uncertainties in emissions and atmospheric aerosol distributions.~~ Historical emission estimates for anthropogenic aerosol and precursor compounds are key data needed for climate and atmospheric chemistry transport models in order to examine how these drivers have contributed to climate change. ~~The historical emission data set used in the Coupled Model Intercomparison Project Phase 5 (CMIP5), important for the IPCC AR5 forcing estimates, covered the period up to 2000.~~ The Community Emissions Data System (CEDS) recently published a new time series of emissions from 1750 to 2014, which will be used in the upcoming CMIP6 [*Hoesly et al.*, 2018]. CEDS includes several improvements ~~over previous inventories~~, including annual temporal resolution with seasonal cycles, consistent methodology between different species, and extending the time series to more recent years ~~[*Hoesly et al.*, 2018]~~, compared to previous inventories and assessments [e.g., *Lamarque et al.*, 2010; *Taylor et al.*, 2012]. During the period from 2000 to 2014, global emissions of black carbon (BC) and organic carbon (OC) have increased, while nitrogen oxide (NOx) emissions have been relatively constant after 2008, and sulfur dioxide (SO$_2$) emissions were back at 2000 levels in 2014, after a temporary increase [*Hoesly et al.*, 2018]. Furthermore, both CEDS and other recent emission inventories report considerably higher estimates of global BC and OC emissions in recent years than earlier inventories [*Granier et al.*, 2011; *Klimont et al.*, 2017; *Lamarque et al.*, 2010; *Wang et al.*, 2014]. The global trend in emissions is driven by a strong increase in emissions from Asia and Africa, and a decline in North America and Europe. Capturing such geographical differences is essential, as the distribution, lifetime and radiative forcing of aerosols depend on their location.

~~The diversity in radiative forcing (RF) estimates also stems from uncertainties in the simulated spatiotemporal distribution of aerosols, their chemical composition and properties.~~ After emission or formation, particles undergo transport, mixing, chemical aging and removal by dry and wet deposition, resulting in a short atmospheric residence time~~lifetime~~, and a highly heterogeneous

99 distribution in space and time. Consequently, accurate representation of ~~the~~ observed aerosols
100 ~~distributions~~ remains challenging, and ~~. P~~previous studies have shown that considerable diversity
101 in the abundance and distribution of aerosols exist between global models. *Bian et al.* [2017] found
102 that the atmospheric burden of nitrate aerosols differ by a factor of 13 between the models in
103 AeroCom Phase III, caused by differences in both chemical and deposition processes. A smaller,
104 but still considerable, model spread in the simulated burden of organic aerosols (OA) from 0.6-3.8
105 Tg was found by *Tsigaridis et al.* [2014]. It was also shown that OA concentrations on average
106 were underestimated. There has been particular focus on BC aerosols over recent years. Multi-
107 model studies have shown variations in global BC burden and lifetime up to a factor of 4-5 [*Lee*
108 *et al.*, 2013; *Samset et al.*, 2014]. Previous comparisons of modeled BC distributions with
109 observations have also pointed to two distinct features common to many models: an overestimation
110 of high altitude concentrations at low- to mid-latitudes and discrepancies in the magnitude and
111 seasonal cycle of high-latitude surface concentrations (e.g., [*Eckhardt et al.*, 2015; *Lee et al.*, 2013;
112 *Samset et al.*, 2014; *Schwarz et al.*, 2013]. As accurate representation of the observed aerosol
113 distributions in global models is crucial for confidence in estimates of radiative forcing (RF), these
114 issues emphasize the need for broad and up-to-date evaluation of model performance.

115 The diversity of simulated aerosol distributions, and discrepancies between models and
116 measurements, stem from uncertainties in the model representation aerosol processing. Knowledge
117 of the factors that control the atmospheric distributions is therefore needed to identify potential
118 model improvements and need for further observational data, and to assess how remaining
119 uncertainties affect the modeled aerosol abundances and, in turn, estimates of RF and climate
120 impact. A number of recent studies have investigated the impact of changes in aging and
121 scavenging processes on

122 ~~Changes to one or more of the abovementioned processes may have considerable impact on the~~
123 ~~simulated concentrations, and propagates to uncertainties in estimates of both RF and climate~~
124 ~~impact. A number of recent studies have investigated possible factors controlling~~ the BC
125 distribution, focusing on aging and wet scavenging processes (e.g., [*Bourgeois and Bey*, 2011;
126 *Browse et al.*, 2012; *Fan et al.*, 2012; *Hodnebrog et al.*, 2014; *Kipling et al.*, 2013; *Lund et al.*,
127 2017; *Mahmood et al.*, 2016]), resulting in notable improvements, at least for specific regions or
128 observational data sets. However, ~~W~~with some~~a few~~ notable exceptions ~~(e.g.,~~ [e.g., *Kipling et al.*,
129 2016]~~)~~, few~~er~~ studies have focused on impacts of scavenging and other processes on a broader set
130 of aerosol species or the combined impact in terms of total aerosol optical depth (AOD).

131 Here we use the CEDS historical emission inventory as input to the chemistry-transport model
132 OsloCTM3 to quantify the change in atmospheric concentrations over the period of 1750 to 2014.
133 The OsloCTM3 is an update of the OsloCTM2, and includes several key changes compared to its
134 predecessor. The significant existing model spread and sensitivity to process parameterizations
135 underlines the need for careful and updated documentation of new model versions, and the
136 increasing amount of available measurement data allows for improved evaluation. Before the
137 model is used to quantify historical time series, we therefore evaluate the simulated present-day

138 aerosol concentrations and optical depth against a range of observations. To get a first-order
139 overview of how uncertainties in key processes and parameters affect the atmospheric abundance
140 and distribution of aerosols in the OsloCTM3, we perform a range of sensitivity simulations. In
141 addition to changes in the scavenging (solubility) assumptions, runs are performed with different
142 emission inventories, horizontal resolution, and meteorological data. The impact on individual
143 species and total AOD, as well as on the model performance compared with observations, is
144 investigated. Finally, we present updated estimates of the historical evolution of radiative forcing
145 due to aerosol-radiation interactions from pre-industrial to present, taking into account recent
146 literature on aerosol optical properties. Section 2 describes the model and methods, while results
147 are presented in Sect. 3 and discussed in Sect. 4. The conclusions are given in Sect. 5.

148

149 2 Methods

150

151 2.1 OsloCTM3

152

153 The OsloCTM3 is a global 3-dimensional chemistry-transport model driven by 3-hourly
154 meteorological forecast data [*Søvde et al.*, 2012]. The OsloCTM3 has evolved from its predecessor
155 OsloCTM2 and includes several updates to the convection, advection, photodissociation and
156 scavenging schemes. Compared with OsloCTM2, the OsloCTM3 has a faster transport scheme, an
157 improved wet scavenging scheme for large scale precipitation, updated photolysis rates and a new
158 lightning parameterization. The main updates and subsequent effects on gas-phase chemistry were
159 described in detail in *Søvde et al.* [2012]. Here we document the aerosols in OsloCTM3, including
160 BC, primary and secondary organic aerosols (POA, SOA), sulfate, nitrate, dust and sea salt. The
161 aerosol modules in OsloCTM3 are generally inherited and updated from OsloCTM2. The
162 following paragraph briefly describes the parameterizations, including updates new to this work.

163

164 The carbonaceous aerosol module was first introduced by *Berntsen et al.* [2006] and has later been
165 updated with snow deposition diagnostics [*Skeie et al.*, 2011]. The module is a bulk scheme, with
166 aerosols characterized by total mass and aging represented by transfer from hydrophobic to
167 hydrophilic mode at a constant rate. In the early model versions, this constant rate was given by a
168 global exponential decay of 1.15 days. More recently, latitudinal and seasonal variation in transfer
169 rates based on simulations with the microphysical aerosol parameterization M7 were included
170 [*Lund and Berntsen*, 2012; *Skeie et al.*, 2011]. Previous to this study, additional M7 simulations
171 have been performed to include a finer spatial and temporal resolution in these transfer rates.
172 Specifically, the latitudinal transfer rates have been established based on experiments with 10
173 instead of four emission source regions and with monthly, not seasonal resolution. In OsloCTM3
174 the carbonaceous aerosols from fossil fuel and biofuel combustion are treated separately, allowing
175 us to capture differences in optical properties in subsequent radiative transfer calculations (Sect.
176 2.4). In contrast to the OsloCTM2, OsloCTM3 treats POAorganic matter (OM) instead of OC. If

177 emissions are given as OC, a factor of 1.6 for anthropogenic emissions and 2.6 for biomass burning
178 sources is used for the OC-to-POA~~OM~~ conversion, following suggestions from observational
179 studies [*Aiken et al.*, 2008; *Turpin and Lim*, 2001]. Upon emission, 20% of BC is assumed to be
180 hydrophilic and 80% hydrophobic, while a 50/50 split is assumed for POA~~OM~~ [*Cooke et al.*, 1999].
181 An additional update in this work is the inclusion of marine primary organic aerosols following
182 the methodology by *Gantt et al.* [2015], where emissions are determined by production of sea
183 spray aerosols and oceanic chlorophyll A. Monthly concentrations of chlorophyll A from the same
184 year as the meteorological data is taken from the Moderate Resolution Imaging Spectroradiometer
185 (MODIS; available from https://modis.gsfc.nasa.gov/data/dataprod/chlor_a.php), while sea spray
186 aerosols are simulated by the OsloCTM3 sea salt module. The climatological annual mean total
187 emission of marine POA~~OM~~ is scaled to 6.3 Tg based on *Gantt et al.* [2015]. The scaling factor
188 depends on the chosen sea salt production scheme (see below) and to some degree on the resolution;
189 here we have used a factor of 0.5.

190 The formation, transport and deposition of SOA are parameterized as described by *Hoyle et al.*
191 [2007]. A two product model (Hoffmann et al., 1997) is used to represent the oxidation products
192 of the precursor hydrocarbons and their aerosol forming properties. Precursor hydrocarbons which
193 are oxidized to form condensable species include both biogenic species such as terpenes and
194 isoprene, as well as species emitted predominantly by anthropogenic activities (toluene, m-xylene,
195 methylbenzene and other aromatics). The gas/aerosol partitioning of semi-volatile inorganic
196 aerosols is treated with a thermodynamic model [*Myhre et al.*, 2006]. The chemical equilibrium
197 between inorganic species (ammonium, sodium, sulfate, nitrate and chlorine) is simulated with the
198 Equilibrium Simplified Aerosol model (EQSAM) [*Metzger et al.*, 2002a; *Metzger et al.*, 2002b].
199 The aerosols are assumed to be metastable, internally mixed and obey thermodynamic gas/aerosol
200 equilibrium. Nitrate and ammonium aerosols are represented by a fine mode, associated with sulfur,
201 and a coarse mode associated with sea salt, and it is assumed that sulfate and sea salt do not interact
202 through chemical equilibrium [*Myhre et al.*, 2006]. The sulfur cycle chemistry scheme and
203 aqueous-phase oxidation is described by *Berglen et al.* [2004].
204
205 The sea salt module originally introduced by *Grini et al.* [2002] has been updated with a new
206 production parameterization following recommendations by *Witek et al.* [2016]. Using satellite
207 retrievals, Witek et al. (2016) evaluated different sea spray aerosol emission parametrizations and
208 found the best agreement with the emission function from *Sofiev et al.* [2011] including the sea
209 surface temperature adjustment from *Jaeglé et al.* [2011]. Compared to the previous scheme, the
210 global production of sea salt is reduced, while there is an increase in the tropics. This will have an
211 impact on the uptake of nitric acid in sea salt particles, consequently affecting NOx, hydroxide
212 (OH) and ozone levels. However, here we limit the scope to aerosols. The Dust Entrainment and
213 Deposition (DEAD) model v1.3 [*Zender et al.*, 2003]was implemented into OsloCTM2 by *Grini*
214 *et al.* [2005] and is also used in OsloCTM3. As a minor update, ~~the DEAD~~ radiative flux~~energy~~
215 ~~budget~~ calculation~~s~~, ~~~~required for determination of boundary layer properties in the dust

216 mobilization parameterization [*Zender et al.*, 2003], now uses radiative surface properties and soil
217 moisture from the meteorological fields.
218
219 Aerosol removal includes dry deposition and washout by convective and large-scale rain. Rainfall
220 Wet scavenging of aerosols is calculated based on European Center for Medium-Range Weather
221 Forecast (ECMWF) data for convective activity, cloud fraction and rain fall, and on the solubility
222 of individual species. The efficiency with which aerosols are scavenged by the precipitation in a
223 grid box is determined by a fixed fraction representing the fraction of this grid box that is available
224 for removal, while the rest is assumed to be hydrophobic. The parameterization distinguishes
225 between For large-scale precipitation in the ice and liquid phase, and the OsloCTM3 has a more
226 complex cloud model than OsloCTM2 that accounts for overlapping clouds and rain based on [*Neu*
227 *and Prather*, 2012] (Neu and Prather 2012). When rain containing species falls into a grid box
228 with drier air it will experience reversible evaporation. Ice scavenging, on the other hand, can be
229 either reversible or irreversible. For further details about large-scale removal we refer the reader
230 to *Neu and Prather* [2012]. Convective scavenging is based on the Tiedtke mass flux scheme
231 (Tiedtke 1989) and is unchanged from the OsloCTM2. The solubility of aerosols is given by
232 constant fractions, given for each species and type of precipitation (i.e., large-scale rain, large-
233 scale ice, and convective) (Table 2). Dry deposition rates are unchanged from OsloCTM2, but the
234 OsloCTM3 includes a more detailed land use dataset (18 land surface categories at 1°x1°
235 horizontal resolution compared to 5 categories at T42 resolution), which affects the weighting of
236 deposition rates for different vegetation categories. Re-suspension of dry deposited aerosols is not
237 treated.
238
239
240 2.2 Emissions
241
242 The baseline and historical simulations use the CEDS anthropogenic [*Hoesly et al.*, 2018; *Smith et*
243 *al.*, 2015] and biomass burning (BB4CMIP) [*van Marle et al.*, 2017] emissions. The CEDS
244 inventory provide monthly gridded emissions of climate-relevant greenhouse gases, aerosols and
245 precursor species from 1750 to 2014 using a consistent methodology over time. Anthropogenic
246 CEDS emissions are comparable to, but generally higher than, other existing inventories [*Hoesly*
247 *et al.*, 2018]. Biogenic emissions are from the inventory developed with the Model of Emissions
248 of Gases and Aerosols from Nature under the Monitoring Atmospheric Composition and Climate
249 project (MEGAN-MACC) [*Sindelarova et al.*, 2014] and are held constant at the year 2010 level.
250 Here we use the CEDS version released in 2016 (hereafter CEDSv16). In May 2017, after
251 completion of our historical simulations, an updated version of the CEDS emission inventory was
252 released after users reported year-to-year inconsistencies in the country/sector level gridded data.
253 The emission totals were not affected, but there were occasional shifts in the distribution within
254 countries (http://www.globalchange.umd.edu/ceds/ceds-cmip6-data/). The potential implications
255 for our simulations are discussed below.

256 Two other emission inventories are also used. The ECLIPSEv5 emission dataset was created with
257 the Greenhouse Gas - Air Pollution Interactions and Synergies (GAINS) model [*Amann et al.*,
258 2011] and provides emissions in 5 year intervals from 1990 to 2015, as well as projections to 2050
259 [*Klimont et al.*, 2017]. The 1990-2015 emission series was recently used to simulate changes in
260 aerosols and ozone and their RF [*Myhre et al.*, 2017]. Here we only use emissions for 2010 in the
261 sensitivity simulation.

262 The Representative Concentration Pathways (RCPs) [*van Vuuren et al.*, 2011] were developed as
263 a basis for near- and long-term climate modeling and were used in CMIP5 and Atmospheric
264 Chemistry and Climate Model Intercomparison Project (ACCMIP) experiments. While the four
265 RCPs span a large range in year 2100 RF, emissions of most species have not diverged
266 significantly in 2010 and we select the RCP4.5 for use here [*Thomson et al.*, 2011]. Table S1
267 summarized total global emissions of BC, OC, NO_x and SO_2 in 2010 in each of the three scenarios.

268 In the simulations with the ECLIPSEv5 and RCP4.5 inventories, biomass burning emissions are
269 from the Global Fire Emission Database Version 4 (GFED4) [*Randerson et al.*, 2017]. The
270 BB4CMIP emissions are constructed with GFED4 1997-2015 emissions as a basis [*van Marle et
271 al.*, 2017] and emissions in 2010 are similar in both datasets. Hence, any difference between the
272 sensitivity simulations stems from differences in the anthropogenic inventory.

273
274
275 2.3 Simulations
276

277 Time slice simulations with CEDSv16 emissions for 1750, 1850 and from 1900 to 2014 are
278 performed (every ten years from 1900-1980, thereafter every five years), one year with ~~including~~
279 six months spin-up. The model is run with year 2010 meteorological data and a horizontal
280 resolution of 2.25x2.25 degrees (denoted 2x2), with 60 vertical layers. While *Søvde et al.* [2012]
281 used meteorological data from the ECMWF IFS model cycle 36r1, we apply here meteorology
282 from the ECMWF OpenIFS cycle 38r1 (https://software.ecmwf.int/wiki/display/OIFS/).
283
284 Additional model runs are performed to investigate the importance of differences in key processes
285 for the aerosol distributions and model performance (Table 1). In addition to the CEDSv16
286 emissions, the model is run with ECLIPSEv5 and RCP4.5 emission inventories for anthropogenic
287 emissions and GFEDv4 biomass burning emissions. Additionally, we perform simulations with
288 1.125x1.125 degrees (denoted 1x1) horizontal resolution. To investigate the importance of
289 meteorology, the simulation with CEDSv16 emissions is repeated with meteorological data for
290 year 2000 instead of 2010. Year 2000 is selected due to its opposite El Niño–Southern Oscillation
291 (ENSO) index compared to 2010. Finally, three model runs are performed with increased and
292 decreased aerosol removal ~~scavenging efficiency~~ by large-scale ice clouds and decreased aerosol
293 scavenging by liquid (large-scale and convective) precipitation. To modify the scavenging, we
294 tune the ~~The efficiency with which aerosols are scavenged by precipitation is determined by a~~

295 ~~fixed fraction representing the fraction of the grid box that is available for removal, while the rest~~
296 ~~is assumed to be hydrophobic.~~ ~~Table 2 summarizes the~~ fixed fractions that control aerosol removal
297 efficiency in the model (see Sect. 2.1). Table 2 summarizes fractions used in the baseline
298 configuration and the three sensitivity tests. A decrease and increase in efficiency of 0.2 is adopted
299 for scavenging of all aerosols by liquid clouds (except hydrophobic BC and POA) and ice clouds,
300 respectively. Note that there is no test with increased removal by liquid clouds, as, with the
301 exception of hydrophobic BC, POA and SOA, 100% efficiency is already assumed. For ice clouds
302 we also reduce the efficiency to a fraction of 0.1, or 0.001 if the value is 0.1 in the baseline
303 configuration. We note that these changes do not represent realistic uncertainty ranges based on
304 experimental or observational evidence, as there are limited constraints in the literature, but are
305 chosen to explore the impact of a spread in the efficiency with which aerosols act as ice and cloud
306 condensation nuclei. ~~in the baseline configuration and the assumptions in the three sensitivity tests.~~
307 ~~*Kipling et al.* [2016]~~ ~~in the baseline configuration and the assumptions in the three sensitivity tests.~~
308

309 2.4 Radiative transfer
310

311 We calculate the radiative forcing of anthropogenic aerosols due to aerosol-radiation interactions
312 (RFari) [*Myhre et al.*, 2013b]). The radiative transfer calculations are performed with a multi-
313 stream model using the discrete ordinate method [*Stamnes et al.*, 1988]. The model includes gas
314 absorption, Rayleigh scattering, absorption and scattering by aerosols, and scattering by clouds.
315 The RFari of individual aerosols is obtained by separate simulations, where the concentration of
316 the respective species is set to the pre-industrial level. The aerosol optical properties have been
317 updated from earlier calculations using this radiative transfer model [*Myhre et al.*, 2007; *Myhre et*
318 *al.*, 2009], in particular those associated with aerosol absorption. The *Bond and Bergstrom* [2006]
319 recommendation of a mass absorption coefficient (MAC) for BC of around 7.5 $m^2 g^{-1}$ for freshly
320 emitted BC and an enhancement factor of 1.5 for aged BC was used previously. In the present
321 analysis, we apply a parametrization of MAC from observations over Europe by *Zanatta et al.*
322 [2016], where MAC depends on the ratio of non-BC to BC abundance. The mean MAC of BC
323 from these observations ~~over Europe is~~ around 10 $m^2 g^{-1}$ at 630 nm [*Zanatta et al.*, 2016]. The
324 measurements in *Zanatta et al.* [2016] represent continental European levels. For very low
325 concentrations of BC, the formula given in *Zanatta et al.* [2016] provides very high MAC values.
326 We have therefore set a minimum level of BC of 1.0e-10 $g m^{-3}$ for using this parameterization, and
327 for lower concentrations we use [*Bond and Bergstrom*, 2006]. In addition, we have set a maximum
328 value of MAC of 15 $m^2 g^{-1}$ (637 nm) to avoid unrealistic high values of MAC compared to
329 observed values. ~~For low aerosol concentrations we apply the approach from *Bond and Bergstrom*~~
330 ~~[2006]. The absorption by organic matter is uncertain [*Bond et al.*, 2013]. Here, we have~~
331 ~~implemented absorbing organic matter according to refractive indices from *Kirchstetter et al.*~~
332 ~~[2004] to 1/3 of the biofuel organic matter and ½ of the SOA from anthropogenic volatile organic~~
333 ~~carbon (VOC) precursors. The remaining fractions of biofuel, fossil fuel and marine POA and~~
334 ~~SOA (anthropogenic and all natural VOCs) are assumed to be purely scattering organic matter.~~

Organic matter has a large variation in the degree of absorption [e.g., Kirchstetter et al., 2004; Xie et al., 2017], from almost no absorption to a strong absorption in the ultraviolet region. Here, we have implemented absorbing organic matter according to refractive indices from Kirchstetter et al. [2004]. The degree of absorption varies by source and region and is at present inadequate quantified: Here we assume 1/3 of the biofuel organic matter and ½ of the SOA from anthropogenic volatile organic carbon (VOC) precursors. The remaining fractions of biofuel, fossil fuel and marine POA and SOA (anthropogenic and all natural VOCs) are assumed to be purely scattering organic matter. As these fractions are not sufficiently constrained by observational data and associated with significant uncertainty, we also perform calculations with no absorption by organic matter.

2.5 Observations

A range of observational datasets are used to evaluate the model performance in the baseline simulation. Note that we use the term "black carbon" in a qualitative manner throughout the manuscript to refer to light-absorbing carbonaceous aerosols. However, when comparing with measurements, we use either elemental carbon (EC) or refractive BC (rBC), depending on whether the data is derived from methods specific to the carbon content of carbonaceous aerosols or incandescence methods, in line with recommendations from *Petzold et al.* [2013].

Measured surface concentrations of EC, OC, sulfate and nitrate are obtained from various netframeworks. For the US, measurements from IMPROVE (Interagency Monitoring of Protected Visual Environments) and CASTNET (Clean Air Status and Trends Network) are used. For Europe, data from EMEP (European Monitoring and Evaluation Programme) [*Tørseth et al.*, 2012] and ACTRIS (Aerosols, Clouds and Trace gases Research InfraStructure) [*Cavalli et al.*, 2016; *Putaud et al.*, 2010] is used. EMEP and ACTRIS sites are all regional background sites, representative for a larger area. To broaden the geographical coverage we also compare the model output against additional observations from the CMA Atmospheric Watch Network (CAWNET) in China [*Zhang et al.*, 2012] and those reported in the literature from India (see *Kumar et al.* [2015] for more details). CASTNET, IMPROVE, EMEP and ACTRIS data is from year 2010, while CAWNET observations were sampled in 2006-2007 and the observational data base from India compiled by *Kumar et al.* [2015] cover a range of years. IMPROVE provides mass of aerosols using filter analysis of measurements of particulate matter with diameter of less than 2.5 micrometers ($PM_{2.5}$), while CASTNET uses an open-face filter pack system with no size restriction to measure concentrations of atmospheric sulfur and nitrogen species [*Lavery et al.*, 2009]. Mass of individual species from the CAWNET network is obtained from aerosol chemical composition analysis performed on PM_{10} samples [*Zhang et al.*, 2012]. EMEP and ACTRIS measurements of EC and OC are in the $PM_{2.5}$ range, whereas nitrate and sulfate measurements are filter-based with no size cutoff limit. Data resulting from EMEP and ACTRIS are archived in the EBAS data base ((http://ebas.nilu.no) at NILU - Norwegian Institute for Air Research, and are openly available (see also Data availability).

375

Modeled AOD is evaluated against the Aerosol Robotics Network (AERONET). AERONET is a global network of stations measuring radiance at a range of wavelengths with ground-based sun-photometers, from which aerosol column burden and optical properties can be retrieved [*Dubovik and King*, 2000; *Holben et al.*, 1998]. The comparison with AERONET data was done using processed through the validation tools available from the AeroCom data base hosted by Met Norway (http://aerocom.met.no/data.html). We also compare against AOD retrievals from MODIS-Aqua and Terra (level 3 atmosphere products, AOD550 combined dark target and deep blue, product version 6) [*MOD08*, 2018] and the Multi-angle Imaging SpectroRadiometer (MISR) (level 2 aerosol product, product version 4) [*MISR*, 2018].

Figure S1 depicts the locations of all the stations. For comparison with surface concentrations and AERONET AOD, the model data is linearly interpolated to the location of each station using annual mean, monthly mean (concentrations) or 3-hourly output (AOD), depending on the resolution of the observations. In the case of AERONET, high mountain stations (here defined as having an elevation higher than 1000 meter above sea level) are excluded following *Kinne et al.* [2013]. For comparison with observed OC surface concentrations, modeled OA is converted to OC using factor of 1.6 for POA and 1.8 for SOA. Unless measurements are restricted to the PM2.5 size range, the comparison includes both fine and coarse mode modeled nitrate (Sect. 2.1). Several statistical metrics are used to assess the model skill, including correlation coefficient (R), root mean square error (RMSE), variance and normalized mean bias (NMB).

The modeled vertical distribution of BC is compared with aircraft measurements of refractory BC (rBC) from the HIAPER Pole-to-Pole Observations (HIPPO) campaign [*Wofsy et al.*, 2011]. Vertical profiles of BC from OsloCTM2 have been evaluated in several previous studies (e.g., *Samset et al.* [2014]) and a more thorough comparison of OsloCTM3 results against a broader set of campaigns is provided by *Lund et al.* [2018]. In the present analysis we focus on data from the third phase (HIPPO3) flights, the only phase that was conducted in 2010, i.e., the same year as our sensitivity simulations. Model data is extracted along the flight track using an online flight simulator. The data is separated into five latitude regions and vertical profiles constructed by averaging observations and model output in 13 altitude bins.

3 Results

We first document the aerosol distributions simulated in the baseline model configuration, focusing on the anthropogenic contribution, and compare with observations, multi-model studies and results from the sensitivity tests. With the present-day model performance evaluated, we then present the updated historical development of RFari of anthropogenic aerosols.

413   3.1 Evaluation of present-day aerosol distributions
414
415   The global mean aerosol burdens and atmospheric residence times (ratio of burden to total wet
416   plus dry deposition) in the baseline simulation are summarized in Table 3 (top row), with spatial
417   distribution shown in Fig. S2. ~~Table S3 also shows the split of OA between secondary and primary~~
418   ~~sources.~~ Compared to results from the AeroCom III experiment, the OsloCTM3 sulfate burden of
419   5.4 mg m^{-2} estimated here is about 50% higher than the multi-model mean of 3.5 mg m^{-2} and 35%
420   higher than OsloCTM2 [*Bian et al.*, 2017]. While the total SO_2 emission is only 5% higher in the
421   present study than in the OsloCTM2 AeroCom III simulation, the atmospheric residence time of
422   sulfate is 50% longer, suggesting that the burden difference is mainly attributable to changes in
423   the parameterization of dry and large-scale wet deposition in OsloCTM3 (Sect. 2.1). The nitrate
424   burden is nearly a factor three higher than both the AeroCom multi-model mean and OsloCTM2
425   burden, and higher than all nine models contributing in AeroCom III [*Bian et al.*, 2017]. This is
426   mainly due to a higher burden of coarse mode nitrate aerosols, associated with less efficient
427   scavenging of sea salt in OsloCTM3 than OsloCTM2. The global budgets of OA simulated by the
428   AeroCom II models was analyzed by *Tsigaridis et al.* [2014]. The burden of OA in the OsloCTM3
429   of 3.4 mg m^{-2} is close to their multi-model mean of 3.1 mg m^{-2} and 25% higher than the OsloCTM2.
430   The OsloCTM3 estimate includes the contribution from marine OA emissions (Sect. 2.1), which
431   may explain part of the difference as. marine OA~~This~~ was included in ~~only~~ some of the AeroCom
432   II models, but ~~and~~ not ~~in~~ OsloCTM2~~, which may partly explain the slightly lower OsloCTM2 OA~~
433   ~~burden in *Tsigaridis et al.* [2014].~~ However, the marine POA only contributes around 3% to the
434   total OA. Additionally, the residence time of OA of 5.3 days is longer than in the OsloCTM2
435   AeroCom II experiment. ~~However, the marine POA only contributes around 3% to the total OA~~
436   ~~(Table S3).~~ The global BC burden of 0.23 mg m^{-2} is also close to the mean of the AeroCom II
437   models of 0.25 mg m^{-2} [*Samset et al.*, 2014]. We note that different emission inventories were used
438   in the AeroCom experiments and the present analysis, however, the comparison shows that the
439   aerosol burdens simulated by OsloCTM3 fall within the range of existing estimates from global
440   models.
441
442   Figure 1 shows results from the baseline OsloCTM3 simulation against annual mean measured
443   surface concentrations of EC, OC, sulfate and nitrate in Europe, North America and Asia ~~against~~
444   ~~output from the baseline OsloCTM3 simulation~~. Overall, the OsloCTM3 shows a high correlation
445   of 0.8-0.9 with measured surface concentrations. There is a general tendency of underestimation
446   by the model, with the lowest NMB and RMSE for BC and nitrate (-23%) and the highest for
447   sulfate (-52%). There are, however, notable differences in model performance between data sets
448   in different regions, as seen from Table S2. For all species, the NMB and RMSE are highest for
449   measurements in China. For instance, excluding the CAWNET measurements, reduces the NMB
450   for sulfate in Fig. 1 from -52% to -31% (not shown). In contrast, the correlation with CAWNET
451   observations is generally similar to, or higher than, other regions/networks. In the case of BC and
452   nitrate, the model slightly overestimates concentrations in Europe and North America, but

453 underestimates Asian measurements. The best overall agreement is generally with IMPROVE
454 observations in North America. Differences in instrumentation between different networks can
455 affect the evaluation. *Lavery et al.* [2009] found that measurements from CASTNET typically gave
456 higher nitrate surface concentrations than values obtained from co-located IMPROVE stations,
457 which could partly explain the NMB of opposite sign in these two networks in Table S2. For BC,
458 we also include measurements from across India compiled by *Kumar et al.* [2015]. This is a region
459 where emissions have increased strongly, but where evaluation of the model performance so far
460 has been limited due to availability of observations. The model underestimates concentrations with
461 a NMB of -43%, however, the correlation of 0.60 is similar to the comparison with data from
462 China and higher than the other regions. An examination of the monthly concentrations (Fig. S3)
463 shows that the largest discrepancies occur during winter, with the largest bias found for
464 measurements in North East India. One possible reason could be missing or underestimated
465 emission sources. This finding is similar to the comparison of measurements against WRF-chem
466 by *Kumar et al.* [2015]. The seasonality of BC concentrations has also been an issue at high
467 northern latitudes, where earlier versions of the OsloCTM strongly underestimated winter and
468 springtime surface concentrations at Arctic stations [*Lund et al.*, 2017; *Skeie et al.*, 2011], similar
469 to many other models [*Eckhardt et al.*, 2015]. This Arctic underestimation persists in the current
470 version of the model. Seasonal differences exist also in other regions, but not consistently across
471 measurement networks. Compared with EC measurements from EMEP/ACTRIS the correlation
472 is poorer during winter and spring, and the model underestimate concentrations in contrast to a
473 positive NMB in summer and fall. However, due to the relatively low number of stations, these
474 values are sensitive to a few stations with larger measurement-model discrepancies. For both
475 IMPROVE and EMEP/ACTRIS, the model underestimation of sulfate is larger during summer
476 and fall, but with opposite seasonal differences in correlation. In general, the number of stations
477 and evaluation of data from only one year limits the analysis of seasonal variations.

478 We do not evaluate ammonium concentrations in the present analysis, as that requires a detailed
479 discussion of the nitrate and sulfate budgets, which has been covered by the recent multi-model
480 ~~nitrate~~ evaluation ~~study~~ by *Bian et al.* [2017] based on an AeroCom Phase III experiment, in which
481 the OsloCTM3 participated. Results showed that~~-~~ most models tend to underestimate ammonium
482 concentrations compared to observations in North America, Europe and East Asia, with a multi-
483 model mean bias and correlation of 0.886 and 0.47, respectively. T~~t~~he OsloCTM3 shows good
484 agreement with ammonium measurements in North America, but has a bias and correlation close
485 the model average in the other two regions. ~~is close to the multi-model mean and similar to the~~
486 ~~other models in terms of agreement with observed ammonium concentrations across USA, Europe~~
487 ~~and East Asia, with an average correlation of 0.47.~~

488 In May 2017, after completion of our historical simulations, an updated version of the CEDS
489 emission inventory was released after an error in the code was reported (see Sect. 2.2). This
490 resulted in occasional shifts in the spatial distribution of emissions within countries with large
491 spatial extent (e.g., USA and China). Since the emission totals were not affected, the impact on

492 our RFari estimates is likely to be small, but shifts in the emission distribution could
493 influenceimpact the model evaluation, in particular for surface concentrations. While repeating all
494 simulations would require more resources than available to us, we have performedrepeated the a
495 year 2010 and 1750 runs. Figure S4 shows the comparison of modeled concentrations against
496 IMPROVE measurements with the limited investigation for the UStwo emission inventory
497 versions, CEDSv16 and CEDSv17., which is one of the regions affected by the emission
498 distribution bug (Fig. S4a). For resource reasons, we limit the analysis to BC, using a model data
499 from one year. We note, however, that the bug is not limited to BC emissions. The comparison
500 against measurements from the IMPROVE network (Fig. S4b-d) In the case of BC, the comparison
501 shows an 5% higher increase in correlation and 15% lower RMSE with the CEDSv17 than
502 CEDSv16. A similar improvement is found for nitrate, with 26% higher correlation and 12% lower
503 RMSE, while in the case of OC and sulfate, the difference is small (< 5%). from 0.33 to 0.43 and
504 a 25 percent reduction in the RMSE when using the May 2017 version of emissions. Smaller
505 differences of between 2-10% are also found in the comparison against measurements in Europe
506 and Asia (not shown). Hence, using the updated version of the emission inventory has an effect on
507 the model performance in terms of surface concentrations, but without changing the overall
508 features or conclusions. The net RFari in 2010 relative to 1750 is 2% stronger with the CEDSv17
509 inventory, a combined effect of slightly higher global BC burden and lower burdens of sulfate and
510 OA.

511 As shown in Table S2, the model overestimate surface concentrations in some regions and
512 underestimate them in others. Compensating biases can influence the evaluation of total AOD.
513 Moreover, the biases differ in magnitude between different species. Moving one step further, we
514 therefore examine the average aerosol composition in the three regions where this is possible with
515 our available measurements. Figure 2 shows the relative contribution from different aerosols
516 species to the total mass in the IMPROVE, EMEP, ACTRIS and CAWNET measurements and the
517 corresponding model results. The number of available aerosol species varies between the
518 measurement networks and we include sea salt from IMPROVE and ammonium from CAWNET.
519 Additionally, the number of stations where simultaneous measurements of all species were
520 available also differ substantially, with 16 for CAWNET, 5 for EMEP/ACTRIS and 172 for
521 IMPROVE. Overall, the relative composition is well represented by the model. The agreement is
522 particularly good for the IMPROVE network. Compared to measurements from CAWNET, the
523 model has a lower relative contribution from OC and more sulfate. In the case of Europe, nitrate
524 aerosols also constitute a significantly larger fraction in the model than in the observations. The
525 evaluation of nitrate is complicated by possible differences in the detection range of
526 instrumentation compared to the size of the two nitrate modes in the model (Sect. 2.1). The
527 comparison against EMEP nitrate data includes both coarse and fine mode modeled nitrate.
528 Excluding the coarse mode, the fraction of total mass attributable to nitrate decreases from 43% to
529 28%, which is much closer to the observed 30% contribution. However, this affects the comparison
530 in Figure 1, resulting in a negative NMB of -34%, compared to -23% when including both coarse
531 and fine mode. This suggest that part, but not all, of the nitrate represented as a coarse mode in the

14

532 model is measured by the instrument, pointing to a need for a more sophisticated size distribution
533 in the model to make better use of available observations. The low number of available stations
534 from EMEP/ACTRISEBAS could also an important factor.

535 Next, we examine total AOD. Figure 3 shows modeled AOD and aerosol absorption optical depth
536 (AAOD), AOD retrieved from MODIS-Aqua and comparison of modeled AOD with AERONET
537 observations. Modeled global, annual mean AOD and AAOD is 0.13 (Fig. 3a) and 0.0051 (Fig.
538 3b), respectively. The overall spatial pattern of modeled AOD agrees well with MODIS (Fig. 3c),
539 however, the latter gives a higher global mean of 0.16 and clearly higher values in North India and
540 parts of China, as well as Central Africa. These peak values are similar to MODIS-Terra, but less
541 pronounced in the AOD retrieved from MISR (Fig. S5), illustrating important differences between
542 different remote sensing products. Nevertheless, an underestimation of modeled AOD in Asia is
543 consistent with results from the evaluation of surface concentrations and can also be seen in the
544 comparison against AERONET, as discussed below. The OsloCTM3 shows a good agreement
545 with measured AOD from the AERONET network, with an overall correlation of 0.82 and RMSE
546 of 0.11, when using monthly mean data from 266 stations (Fig. 3d). Note that the modeled global
547 mean AOD is 0.13, but the model mean at the AERONET stations is 0.175 (Fig 3d) and has only
548 a NMB of -11.8%. Many of the AERONET stations tend not to be regional background sites, but
549 can be influenced by local pollution (e.g., *Wang et al.* [2018])

550 However, as for surface concentrations, there are notable regional differences in model
551 performance. Fig. S6 compares modeled AOD against AERONET stations in Europe, North
552 America, India and China separately. The best agreement is found for Europe and North America,
553 with NMB of -0.4% and -13%, respectively, and RMSE of approx. 0.05. The correlation is higher
554 for North America (0.71) than Europe (0.63). A relatively high correlation of 0.71 is also found
555 for stations in China. However, the NMB and RMSE is higher (-34.5% and 0.25). There are
556 significantly fewer observations for comparison with modeled AOD over India, but the ones
557 available give NMB and RMSE on the same order of magnitude as for China, but a lower
558 correlation (0.45).

559 Ground-based measurements can also provide information about column absorption aerosol
560 optical depth (AAOD). Such information has been used to constrain the absorption of BC and
561 provide top-down estimate of the direct BC RF (e.g., [*Bond et al.*, 2013]). However, retrieval and
562 application of AERONET AAOD is associated with a number of challenges and uncertainties (e.g.,
563 [*Samset et al.*, 2018]), hence such an evaluation is not performed here.

564 Recent literature has pointed to important representativeness errors arising when constraining
565 models using observations due to the coarse spatial and temporal scales of global models compared
566 with the heterogeneity of observations. *Schutgens et al.* [2016a] found differences in RMSE of up
567 to 100% for aerosol optical thickness when aggregating high resolution model output over grid
568 boxes representative of the resolution of current global models compared to small areas
569 corresponding to satellite pixels. Smaller, but notable, differences of up to 20% were found when

570 monthly mean model data was used, as in the present analysis. However, that did not account for
571 issues related to temporal collocation, which can also introduce considerable errors [*Schutgens et*
572 *al.*, 2016b]. In a recent study, *Wang et al.* [2018] found a spatial representativeness error of 30%
573 when constraining AAOD modeled at a 2°x2° horizontal resolution against AERONET retrievals.
574 However, further work is needed to investigate whether similar biases exist for AOD.

575

576 3.2 Sensitivity of aerosols distributions to model input and process parameterization

577

578 As shown in the section above, the OsloCTM3 performs well compared against observed AOD.
579 Still, a number of factors influence the simulated distributions of individual aerosol species. To
580 assess the importance of key uncertainties for modeled distributions and model performance, we
581 perform a range of sensitivity simulations (Table 1) to examine the importance of emission
582 inventory, scavenging assumptions (Table 2), meteorological data and resolution for the modeled
583 aerosol distributions and model performance.

584

585 Global aerosol burdens and AOD in each sensitivity run are summarized in Table 3 (corresponding
586 atmospheric residence times are given in Table S3). The BC burden is particularly sensitive to
587 reduced scavenging by large-scale ice clouds (LSIDEC), resulting in a 40% higher burden
588 compared to the baseline. In contrast, an equal increase in the scavenging efficiency (LSIINC)
589 result in a decrease in burden of only 9%, while decreased scavenging by liquid precipitation
590 (SOLDEC) gives a 13% higher burden. The lower BC emissions in the ECLv5 and CMIP5
591 inventories give a global BC burden that is 9 and 22% lower, respectively. For sulfate, ammonium
592 and OA, we also find the largest burden changes in the LSIDEC case, followed by SOLDEC. The
593 change in the LSIDEC is particularly large for OA and is driven by changes in SOA. For SOA, the
594 changes are determined not only by modifying the scavenging, but also by changes in POA
595 concentrations, which gas-phase secondary organics can partition onto. Increasing the horizontal
596 resolution results in a slightly higher burden for all species, except sea salt.

597 While sensitivity tests may give similar changes in the total global burdens, the spatial distribution
598 of changes can differ substantially. Figure 4 shows the ratio of AOD and total burden by species
599 and altitude in each sensitivity simulation to the baseline. As expected, varying the emission
600 inventories results in changes that are largely confined to the main source regions (Figs.4a,b).
601 Using the CMIP5 inventory results in considerably lower concentrations over Asia, the Middle
602 East and North Africa, reflecting the higher emissions in the more recent inventory. Over ~~Europe~~
603 ~~and most of~~ central North America the AOD ~~re is an increase~~is higher, mainly due to more
604 ~~particularly for sulfate,~~ ammonium nitrate ~~and ammonium~~, whereas the higher AOD over Eastern
605 Europe and part of Russia is a result of higher sulfate concentrations.~~.~~ Similar characteristics ~~A~~
606 ~~similar pattern is~~are found when using ECLv5, but the relative differences are smaller. Reducing
607 or increasing the large-scale ice cloud scavenging gives the largest relative changes in ~~increases~~
608 AOD~~aerosol burdens the most~~ at high latitudes, while changes in the solubility assumption for

liquid precipitation~~clouds~~ affects AOD ~~burdens~~ most~~ly~~ over Asia, where aerosol burdens ~~emissions~~ are high~~est~~, and around the equator where convective activity is stronge~~r~~. In general, the burden of BC, OA and dust is significantly affected by changes in the scavenging assumptions, while nitrate responds more strongly to different emission inventories, likely due to the complicated dependence on emissions of several precursors and competition with ammonium-sulfate. We also note that at higher altitudes the absolute differences in the burden of nitrate are small. Changes in AOD~~burdens~~ resulting from ~~when~~ using different meteorological input data ~~from a different year~~ are more heterogeneous and are most notable in ~~mainly occur in~~ regions where ~~the~~ effects~~influence~~ of choosing data from years with opposite ~~of differences in the~~ ENSO phase are~~is~~ expected ~~to be the main factor~~, e.g., west coast of South America and ~~,~~South East Asia ~~and Australia~~. There is also a notable change in the Atlantic Ocean, where mineral dust is a dominating species. The meteorological data can affect production, deposition and transport of dust directly, as well as indirectly through ENSO-induced teleconnections as suggested by e.g., *Parhi et al.* [2016].

For BC, OA and dust, the largest impact relative to the baseline are seen above 600 hPa in the LSIDEC case. Change in LSIDEC are also important in the case of sulfate and sea salt, but occur at lower altitudes. In contrast to the other aerosol species, differences in emission inventories are most important for nitrate. In a recent study, *Kipling et al.* [2016] investigated factors controlling the vertical distribution of aerosols in the HadGEM3-UKCA. It was found that in-cloud scavenging was very important in controlling the vertical mass concentration of all species, except dust. For dust, it was also found that dry deposition and sub-cloud processes played key roles, processes not examined in the present analysis. Moreover, *Kipling et al.* [2016] performed sensitivity simulations by switching transport and scavenging on and off to get the full effect of a given process, while we perform smaller perturbations to investigate uncertainties. Here we find significant impacts of changes in ice-cloud removal efficiency (Table 2) on the vertical distribution of BC, OA and dust, while large-scale liquid and convective precipitation is more important for sea salt and nitrate

~~With the exception of different emission inventories, there is generally a small impact on near-surface concentrations in near-surface regions compared to the changes in remote areas. This is important to note due to the role of aerosols in air quality perspectives, where uncertainties in near-source concentrations are vital.~~

Our sensitivity tests show that changes in input data, resolution or scavenging can lead to notable changes in the aerosol distributions. The next question is then how these changes affect model performance compared to observations. Figure 5a compares modeled and measured surface concentrations of BC, OC, sulfate and nitrate in each simulation using all observations in Fig. 1. For BC, the sensitivity tests have little or no impact on correlation, but there is a markedly better agreement in terms of standard deviation (i.e., model becomes closer to observations) for CEDSv16/CMIP6 compared to RCP/CMIP5, reflecting the higher emissions in the former. Similar, but smaller, effects are also found for the other species. The improvement from RCP/CMIP5 to

648 CEDSv16/CMIP6 is especially seen for measurements in Asia. A higher resolution is also found
649 to reduce the bias, in particular for BC. Figure 5b shows the comparison against AERONET AOD
650 in each sensitivity simulation. Again, there is a higher correlation and lower bias in the 1x1RES
651 run than in the baseline, while the opposite is found in the RCP/CMIP5 and ECLv5 cases. For both
652 observables, the improvement in the 1x1RES simulation may result from a better sampling at a
653 finer resolution, improved spatial distribution or a combination. The most pronounced changes
654 results from using meteorological data from year 2000, in which case the correlation is reduced
655 from around 0.8 to 0.7.

656 For both observables, the difference in model performance between the baseline and scavenging
657 sensitivity tests is small. This may partly be an effect of the geographical coverage of stations; the
658 majority of measurements are from stations in more urban regions, whereas simulated burden
659 changes occur in remote regions, particularly at high latitudes and altitudes (Fig. 4). We therefore
660 also perform evaluations against AOD from regional sub-sets of AERONET stations. Ten of the
661 AERONET stations used in the present analysis are located north of 65°N (Fig. S1). A comparison
662 of monthly mean simulated AOD in each of the sensitivity runs against observations in this region
663 shows the best agreement with the baseline simulation and with the ECLv5 emission inventory,
664 with a considerably higher bias when scavenging parameters are modified (Fig. S7a). This is
665 particularly the case in the LSIDEC run, where concentrations of all species increase at high
666 latitudes compared to the baseline (Fig. 4). In contrast, the reduced concentrations in LSIINC,
667 results in a negative bias. We note that most of these stations have missing values in the winter
668 months, which is when the model underestimate BC concentrations in the Arctic, hence limiting
669 the evaluation. Decreased scavenging efficiency also leads to a higher bias than in the baseline for
670 observations in Europe and North America (not shown). In Asia, where the model already
671 underestimates aerosols in the baseline configuration, the bias is reduced since concentrations
672 increase. However, differences are smaller than north of 65°N. Moreover, given the notable
673 exacerbation in model performance in other regions, it is likely that other sources of uncertainty
674 (e.g., emissions) are more important for the model-measurement discrepancies in Asia. A similar
675 comparison is performed for 15 AERONET stations located in North Africa and the Middle East
676 (Fig. S7b), where the dust influence is strong. Changing the meteorological year and reducing
677 scavenging results in higher dust burdens (Table 3). Again, the agreement is better in the baseline
678 run than in these sensitivity runs. In particular, the METDATA run result in a higher bias and a
679 lower correlation, which is not surprising as dust production depends also on meteorological
680 conditions. The changes compared to the baseline CEDSv16/CMIP6 simulation cannot be entirely
681 attributed to differences in dust concentrations, as seen from the RCP/CMIP5 and ECLv5
682 simulations where the dust production is equal to the baseline. Several studies have pointed to the
683 importance of spatial resolution for improved model performance compared to observations (e.g.,
684 [*Sato et al.*, 2016; *Schutgens et al.*, 2017; *Schutgens et al.*, 2016a; *Wang et al.*, 2016]). *Wang et al.*
685 [2016] found significant reductions in NMB of BC AAOD relative to AERONET when using a
686 high resolution (10 km) emission data and model output. In our analysis, moving from 2°x2° to
687 1°x1° horizontal resolution also results in a slightly higher correlation and reduced bias and errors

18

688 when compared to all AERONET stations (Fig. 5b). The impact is largest for AOD in China and
689 India, the NMB is reduced (from -34% and -24% (Fig. S6) to -20% and -10%, respectively).
690 However, the opposite effect is found for AERONET stations in Europe and North America. Of
691 course, the 1°x1° resolution is still very coarse compared to the grid sizes used in the
692 abovementioned studies.

693 Changes away from near-source areas are also evaluated in terms of BC concentrations by a
694 comparison with observed vertical distribution from the HIPPO3 campaign, where remote, marine
695 air over the Pacific was sampled across all latitudes (Sect. 2.5). To limit the number of model runs,
696 we focus on only one phase of the HIPPO campaign here, but a more comprehensive evaluation
697 of OsloCTM3 vertical BC distribution against aircraft measurements was performed by [*Lund et*
698 *al.*, 2018]. Figure 6 shows observed average vertical BC concentration profiles against model
699 results from each sensitivity test. The OsloCTM3 reproduces the vertical distribution well in low
700 and mid-latitudes over the Pacific in its baseline configuration, although near-surface
701 concentrations in the tropics are underestimated. This is a significant improvement over the
702 OsloCTM2, where high-altitude concentrations in these regions typically were overestimated. The
703 baseline configuration of OsloCTM3 includes updates to the scavenging assumptions based on
704 previous studies investigating reasons for the high-altitude discrepancies (e.g., [*Hodnebrog et al.*,
705 2014; *Lund et al.*, 2017]. At high northern and southern latitudes, the model underestimates the
706 observed vertical profiles in the baseline. Increasing the model resolution does not have any
707 notable impact on the vertical profiles. There is a notable increase in high-latitude concentrations
708 when large-scale ice cloud scavenging is decreased. However, there is a simultaneous exacerbation
709 of model performance in the other latitude bands, pointing to potential tradeoffs when tuning
710 global parameters, as also illustrated by *Lund et al.* [2017]. Due to the significant altitude
711 dependence of the radiative effect of BC (e.g., [*Samset et al.*, 2013]), high altitude overestimations
712 will contribute ~~significantly~~ to uncertainties in BC RFari. We also note that HIPPO3 was
713 conducted in March/April: Comparison with aircraft measurements from other seasons show a
714 smaller underestimation at high latitudes ([*Lund et al.*, 2018].

715 3.3 Pre-industrial to present-day aerosols
716

717 With confidence in the model ability to reasonably represent current aerosol distributions
718 established, we next present an updated historical evolution of anthropogenic aerosols from pre-
719 industrial to present-day, and the consequent direct radiative effect (RFari) (Sect. 2.4). Figure 7
720 shows the net change in total aerosol load from 1750 to 2014. Full times series by species are given
721 in Table S4. To keep in line with the terminology used in the IPCC AR5, we now separate out
722 biomass burning BC and POA in a separate species "biomass". We also note that only the fine
723 mode fraction of nitrate contributes to the RFari and is inlcuded in Fig. 7. To illustrate the
724 contributions from additional emissions during the past 14 years, we also include the 2000-1750
725 difference. The values from the present study are also compared with results from the AeroCom

726   II models [*Myhre et al.*, 2013a], where emissions over the period 1850 to 2000 from *Lamarque et*
727   *al.* [2010] were used.

728

729   The most notable difference compared to the AeroCom II results is seen for biomass aerosols.
730   Biomass burning emissions have high interannual variability and this affects the analysis. While
731   the 1750-2014 difference is 0.23 mg m^{-2}, taking the difference between year 1750 and 2000 (black
732   asterisk) results in a net change of only 0.03 mg m^{-2}. There is also a much larger change in the
733   burden of biomass aerosols in the AeroCom experiments, reflecting a more than 100% higher
734   emissions in 2000 compared to 1850 *Lamarque et al.* [2010] inventory. However, biomass aerosols
735   comprises both scattering OA and absorbing BC and, as seen below, these nearly cancel in terms
736   of RFari. Changes in sulfate and OA from pre-industrial to 2000 are slightly higher in the present
737   analysis than in AeroCom II, and the influence of additional emissions since 2000 is seen. The
738   OsloCTM3~~fast~~ is well below the AeroCom multi-model mean for nitrate. The OsloCTM2 was
739   found to be in the low range, but the multi-model was also influenced by some models giving high
740   estimates [*Myhre et al.*, 2013a]

741   Using the CEDSv16 emissions, we estimate a ~~total~~ net RFari from all anthropogenic aerosols in
742   2014 relative to 1750 of -0.17 W m^{-2}. The RFari from sulfate is -0.30 W m^{-2}, while the
743   contributions from OA (combined fossil fuel plus biofuel POA and SOA), nitrate and biomass
744   aerosols are smaller in magnitiude of -0.09, -0.02 and -0.0004 W m^{-2}, respectively. The RFari due
745   to fossil fuel and biofuel BC over the period is 0.31 W m^{-2}.

746   Figure 8a shows the time series of RFari by component, as well as the ~~total~~ net, in the present
747   analysis (solid lines), and corresponding results reported in the IPCC AR5 (dashed lines). The net
748   RFari over time is mainly determined by the relative importance of compensating BC and sulfate
749   RFari. The most rapid increase in BC RFari is seen between 1950 and 1990, as emissions in Asia
750   started to grow, outweighing reductions in North America and Europe [*Hoesly et al.*, 2018]. After
751   a period of little change between 1990 and 2000, the rate of change increases again over the past
752   two decades, following strong emission increases in Asia and South Africa. Similarly, cooling
753   contribution from sulfate aerosols strenghtened from around mid-century. However, in contrast to
754   BC, the evolution is fairly flat after 1990. The last 20 years has seen a continuous reduction in
755   sulfur dioxide (SO$_2$) emissions in Europe, from around 30 to 5 Tg yr^{-1} in CEDSv16, with a similar
756   trend in North America. While emissions in China continue to increase well into the 2000s, a
757   stabilization is seen after 2010, following introduction of stricter emission limits as part of a
758   program to desulfurize power plants [*Klimont et al.*, 2013]. During the same period, emissions in
759   India have risen. However, the net global SO$_2$ emission trend over the past few years is a slight
760   decline [*Hoesly et al.*, 2018]. This development is reflected in the net RFari, which reaches its peak
761   (i.e., strongest negative value) around 1990 and gradually becomes weaker thereafter. This trend
762   is more pronounced in the present analysis that in the IPCC AR5 estimates, where the forcing due
763   to sulfate is more flat in recent decades, suggesting that projected emission estimates
764   underestimated recent decreases in SO$_2$. The minimum net RFari value is also reached later in the

765 latter. Moreover, a recent study suggests that current inventories underestimate the decline in
766 Chinese SO_2 emissions and estimate a 75% reduction since 2007 [*Li et al.*, 2017]. In this case, the
767 weakening trend could be even stronger than estimated here. The insert in Fig. 8a focuses on recent
768 estimates of total RFari over the period 1990-2015. Using the ECLv5 emission inventory, *Myhre*
769 *et al.* [2017] found a global mean RFari due to changes in aerosol abundances over the period
770 1990-2015 of 0.05 (±0.04) W m^{-2}. Our results using CEDSv16 emissions are in close agreement
771 with these findings.

773 Over the past decades, there has been shift in emissions, from North America and Europe to South
774 and East Asia. ThisThe geographical shift in emissions is clearly is also reflected in the zonally
775 averaged net RFari over time in Fig. 8b. RFari declined in magnitude north of 40°N after 1980,
776 with particularly large year-to-year decreases between 1990 and 1995, and from 2005 to 2010,
777 and . The RFari has strengthened in magnitude between 10°-30°N in both hemispheres. The RFari
778 also strengthened in the Southern Hemisphere subtropical region, reflecting incresing emission in
779 Africa and South America after 1970. However, , although the peak net RFari around 35°N is
780 considerably weaker in 2014 than the peak in 1980. This mainly is due to fact that simultaneously
781 with the southwards shift, the sulfate burden has declined, while the BC burden has increased
782 steadily at the same latitudes, resulting in a weaker net RF. The past decade, the net RFari has
783 switched from negative to positive north of 70°N, due to a combination of stronger positive RF of
784 BC and from biomass burning aerosols.

786 Table S5 shows changes in burden, AOD, AAOD, RFari, and normalized RF over the period 1750-
787 2010 for individual aerosol components and the net RFari. Compared to earlier versions of
788 OsloCTM [*Myhre et al.*, 2009; *Myhre et al.*, 2013a] the normalized RF with respect to AOD is
789 lower because of short lifetime of BC resulting in smaller abundance of BC above clouds, whereas
790 normalized RF with burden is comparable to earlier estimates because of higher MAC compensate
791 for short lifetime of BC. Weaker normalized RF of OA (POA and SOA) than earlier OsloCTM
792 versions is due to the inclusion of absorbing OA.

794 In the present studyHere we have used an updated parameterization of BC absorption based on
795 *Zanatta et al.* [2016] (Sect. 2.4), which takes into account the ratio of non-BC-to-BC material and
796 results in a MAC of 12.5 m^2 g^{-1} at 550 nm. This is 26% higher than the 9.94 m^2 g^{-1} using the
797 approach from *Bond and Bergstrom* [2006]. Using the latter, we estimate a BC RFari in 2014
798 relative to 1750 of 0.23 W m^{-2}, 25% lower than the 0.31 W m^{-2} calculated based on *Zanatta et al.*
799 [2016]. These results emphasize the importance of assumptions and uncertainties related to the BC
800 absorption.

801 The magnitude of RFari by scattering aerosols is sensitive to assumptions about absorption by
802 organic aerosols, so-called brown carbon (BrC). Observational studies have provided evidence for
803 the existence of such particles, and modeling studies suggest they could be responsible for a
804 substantial fraction of total aerosol absorption, although the spread in estimates is wide (e.g., *Feng*

805   *et al.* [2013] and reference therein). In the present study we assume a considerable fraction of
806   absorption by OA (Sect. 2.4). Assuming purely scattering aerosols, the RFari from OA is -0.13W
807   m^{-2}; acounting for BrC absorption this is weakened to -0.09 W m^{-2}. Splitting total OA RFari into
808   contributions from primary and secondary aerosols, we find that purely scattering POA gives a
809   RFari of -0.07 W m^{-2} compared to -0.06 Wm^{-2} with absorption. The corresponding numbers for
810   SOA are -0.06 and -0.03 W m^{-2}. This indicates that in OsloCTM3, the absorbing properties of SOA
811   are relatively more important than for POA. This is likely due to the generally higher altitude of
812   SOA than POA (Fig. S8) in combination with the increasing radiative efficiency of absorbing
813   aerosols with altitude [*Samset et al.*, 2013]. However, due to the weaker overall contributions from
814   OA, our results indicate that differences in parameterization of BC absorption can be more
815   important than uncertainties in absorption by BrC for the ~~total~~ net RFari.
816

817   4 Discussion
818

819   Our estimate of total net RFari in 2014 relative to 1750 is weaker in magnitude than the best
820   estimate for the 1750-2010 period reported by IPCC AR5. The difference is due to a combination
821   of factors, including weaker contributions from both cooling aerosols and BC. ~~A significant range~~
822   ~~from -0.6 to -0.13 W m^{-2} surrounds the central RFari estimate of -0.35 W m^{-2} from IPCC AR5~~
823   ~~[*Boucher et al.*, 2013], due to the large spread in underlying simulated aerosol distributions. As~~
824   ~~shown in Sect. 3, the OsloCTM3 generally lies close to or above the multi-model mean of~~
825   ~~anthropogenic aerosol burdens from recent studies and performs reasonably well compared with~~
826   ~~observations and other global models, with improvements over the predecessor OsloCTM2.~~
827   ~~In particular, recent progress towards constraining the vertical distribution of BC concentrations~~
828   ~~has resulted in improved agreement between modeled and observed vertical BC profiles over the~~
829   ~~Pacific Ocean with less of the high-altitude overestimation seen in earlier studies. However, as~~
830   ~~shown by *Lund et al.* [2018], discrepancies compared to recent aircraft measurements over the~~
831   ~~Atlantic Ocean remain. The higher emissions in the CEDSv16 inventory also results in an~~
832   ~~improved agreement with BC surface concentrations over Asia.~~ Despite considerably higher BC
833   emissions in the CEDSv16 inventory~~these considerably higher emissions~~ compared to older
834   inventories, we calculate a weaker BC RFari than reported in AR5, hence going in the opposite
835   direction of explaining the difference to IPCC AR5 total RFari. The IPCC AR5 best estimate for
836   fossil fuel and biofuel BC of 0.4 (0.05 to 0.8) W m^{-2} [*Boucher et al.*, 2013] was based mainly on
837   the two studies by *Myhre et al.* [2013a] and *Bond et al.* [2013], who derived estimates of BC RFari
838   of 0.23 (0.06 to 0.48) W m^{-2} and 0.51 (0.06 to 0.91) W m^{-2}, respectively. The spread between the
839   two is largely attributed to methodological differences: *Bond et al.* [2013] used an observationally
840   weighted scaling of results to match those based on AERONET AAOD, which was not adopted
841   by *Myhre et al.* [2013a]. Such ad-hoc adjustments typically result in higher estimates (*Wang et al.*
842   [2018] and references therein). Moreover, a recent study by *Wang et al.* [2018] suggest that
843   representativeness error arising when constraining coarse resolution models with AERONET
844   AAOD could result in a 30% overestimation of BC RFari, which explains some of the differences

845 between bottom-up and observationally constrained numbers. The BC RFari estimate from the
846 present study is around 20% higher than the AeroCom multi-model mean from *Myhre et al.* [2013a]
847 when calculated over the same period 1850-2000. This reflects the higher emissions in the
848 CEDSv16 emission inventory than in *Lamarque et al.* [2010], as well as a higher MAC.

849

850 A significant range from -0.85 to +0.15 W m^{-2} surrounds the central RFari estimate of -0.35 W m^{-2}
851 from IPCC AR5 [*Boucher et al.*, 2013], caused by the large spread in underlying simulated
852 aerosol distributions. Deficiencies in the ability of global models to reproduce atmospheric aerosol
853 concentrations can propagate to uncertainties in RF estimates. As shown in Sect. 3, the OsloCTM3
854 generally lies close to or above the multi-model mean of anthropogenic aerosol burdens from
855 recent studies and is found to performs reasonably well compared with observations and other
856 global models, with improvements over the predecessor OsloCTM2.
857 In particular, recent progress towards constraining the vertical distribution of BC concentrations
858 has resulted in improved agreement between modeled and observed vertical BC profiles over the
859 Pacific Ocean with less of the high-altitude overestimation seen in earlier studies. However, as
860 shown by *Lund et al.* [2018], there are discrepancies compared to recent aircraft measurements
861 over the Atlantic Ocean remain. A remaining challenge is the model underestimation of Arctic BC
862 concentrations. However, this is seen mainly during winter and early spring, when the direct
863 aerosol effect is small due to lack of sunlight. In contrast, the higher emissions in the CEDSv16
864 inventory also results in an improved agreement with BC surface concentrations over Asia. The
865 higher emissions in the CEDSv16 inventory also results in an improved agreement with BC surface
866 concentrations over Asia
867 In general, we find lower surface sulfate concentrations in the model compared with measurements.
868 This could contribute to an underestimation of the sulfate RFari, which is weaker in the present
869 study than in IPCC AR5. An underestimation of observed AOD in Asia is also found, however,
870 the implication of this bias on RF is not straightforward to assess, as it is complicated by the mix
871 of absorbing and scattering aerosols. We also note that the global mean sulfate burden is higher in
872 the OsloCTM3 than in most of the global models participating in the AeroCom III experiment
873 (Sect. 3.1, *Bian et al.* [2017]), and that . Compared with other AeroCom Phase III models, the
874 OsloCTM3 performs similarly to or better than other AeroCom Phase III models in terms of nitrate
875 and sulfate surface concentrations, at least for measurements from CASTNET [*Bian et al.*, 2017].
876 Nevertheless, the model diversity in simulated nitrate and sulfate remains large and, although all
877 models capture the main observed features in concentrations, further work is needed to resolve the
878 differences and improve model performance for these species.

879

880 While a comprehensive quantitive uncertainty analysis of the updated RFari estimate is not
881 possible within the scope of this study, we explore the order of magnitude uncertainties due to
882 "internal" factors such as scavenging parameterizations and model resolution by performing
883 sensitivity tests. Changes in global burden on the order of 10-20%, and up to 65%, were found
884 (Sect. 3.2). However, compared to observations of surface concentrations in near-source regions,

885 total AOD and vertical distribution of BC concentrations, we saw that the model generally
886 performed the best in its baseline configuration. Furthermore, the largest changes in the simulated
887 AOD and aerosol distributions were found in high-latitude regions, whereas changes over land
888 where the concentrations, and hence subsequent RF is localized, were smaller. For certain regions
889 and observables, there were notable differences between the baseline and sensitivity simulations.
890 For instance, an improvemet in the baseline compared to using the CMIP5 emission inventory was
891 seen for BC surface concentrations, in particular in Asia, while the NMB of AOD compared to
892 AERONET stations in the same region was reduced in the simulation with higher spatial resolution.
893 The importance of using the correct meteorological year was also seen. Such uncertainties will
894 translate to the RFari estimates, along with uncertainties in optical properties such as absorption
895 by organic aerosols and parameterization of BC absorption (Sect. 3.3).
896
897 Estimates of radiative impacts depend critically on the confidence in the emission inventories. A
898 detailed discussion of uncertainties in the CEDS inventory is provided by *Hoesly et al.* [2018]. On
899 a global level, the uncertainty in SO_2 emissions tend to be relatively low, although there is an
900 indication of missing SO_2 sources in particular in the Persian Gulf [*McLinden et al.*, 2016], whereas
901 emission factors for BC, OC, NOx, CO and VOCs have higher uncertainties. Uncertainties in
902 country-specific emissions can also be much larger, which is particularly true for carbonaceous
903 aerosols. In future CEDS versions, a quantitative uncertainty analysis is planned [*Hoesly et al.*,
904 2018], which will provide valuble input to modeling studies.
905
906 Our study does not include anthropogenic dust, i.e., wind-blown dust from soils disturbed by
907 human activities such as land use practices, deforestation and agriculture, and fugitive combustion
908 and industrial dust from urban sources. These sources could contribute an important fraction of
909 emissions and ambient $PM_{2.5}$ concentrations in some regions [*Paul et al.*, 2012; *Sajeev et al.*, 2017],
910 but are missing from most models today. For instance, a recent study found a 2–16 mg m^{-3} increase
911 in PM2.5 concentrations in East and South Asia from anthropogenic fugitive, combustion, and
912 industrial dust emissions. However, the transport processes and optical properties, and hence,
913 radiative impact, is poorly known. We also do not include the effect of aerosol-cloud interactions,
914 which are crucial for the net climate impact of aerosols. For instance, recent studies suggest that
915 the impact of BC on global temperature response is small due to largely compensating direct and
916 rapid adjustment ~~semi-direct~~ effects [*Samset and Myhre*, 2015; *Stjern et al.*, 2017]. The
917 composition and distribution of aerosols and oxidants in the pre-industrial atmosphere is uncertain
918 and poorly constrained by observations. However, while this is an important source of uncertainty
919 in estimates of RF due to aerosol-induced cloud albedo changes, it is less important for RFari
920 because the forcing scales quite linearly with aerosol burden [*Carslaw et al.*, 2017].
921
922

5 Conclusions

In this study, we have documented the third generation of the Oslo chemical transport model (OsloCTM3) and evaluated the simulated distributions of aerosols, including results from a range of simulations to investigate the sensitivity to uncertainties in scavenging processes, input of emissions and meteorological data and resolution. We have then used the new historical CEDS emission inventory (version 2016; CEDSv16), which will also be used in the upcoming CMIP6, to simulate the temporal evolution of atmospheric concentrations of anthropogenic aerosols, and quantified the temporal evolution of the subsequent radiative forcing due to aerosol-radiation interactions (RFari).

The total AOD from the OsloCTM3 is in good agreement with observations from the AERONET network with a correlation of 0.82 and a normalized mean bias (NMB) of -11.8%. Regionally, the underestimation of observed AOD is higher for stations in China and India than in Europe and North America, as also reflected from the comparison against measured aerosol surface concentrations. High correlations 0.80-0.90 are also found for surface concentrations of BC, OC, sulfate and nitrate aerosols compared with all measurements across Europe, North America and Asia. The corresponding NMB range from -23% for BC and nitrate to -46% and -52% for OC and sulfate, respectively. The OsloCTM3 performs notably better than its predecessor OsloCTM2 in terms of high-altitude BC distribution as compared with observed BC concentration profiles over the Pacific Ocean from the HIPPO3 campaign. In constrast, the model continues to underestimate observed surface levels of BC during winter and spring. Compared with other recent estimates of aerosol burdens, the OsloCTM3 generally lies close to or above the mean of other global models.

Increasing or reducing the scavenging efficiency, moving to a finer resolution, and using the wrong meteorological year or a different emission inventory results in changes in the global mean aerosol burdens of up to 65%. The burdens of BC, OC and sulfate are particularly sensitive to a reduced efficiency of removal by large-scale ice clouds; a 10 percentage point reduction increases the global burden by 40%, 65% and 20%, respectively. A corresponding increase in the efficiency gives around 10% lower burdens. A significantly better agreement with BC surface concentrations is found when using the CEDSv16 emission inventory compared with the RCP4.5. Furthermore, a notable reduction in the bias of AOD compared to AERONET observations in Asia is found when increasing the horizontal resolution, while the correlation is reduced when using the wrong meteorological year. However, we find no clear evidence of consistently better model performance across all observables and regions in the sensitivity tests than in the baseline configuration. This may in part be influenced by the geographical coverage of observations, as the largest differences in concentrations and AOD from the baseline is found at high altitudes and latitudes where the availability of constraining measurements is limited.

Using the CEDSv16 historical emission inventory we estimate a total net RFari from all anthropogenic aerosols, relative to 1750, of -0.17 W m^{-2}. This is significantly weaker than the best

estimate reported in the IPCC AR5, due to a combination of factors resulting in weaker contributions from both cooling aerosols and BC in our simulations. Our updated RFari estimate is based on a single global model. As shown by previous studies, there is a large spread estimates of RFari due to the spread in modeled aerosol distributions. The present analysis shows that uncertainties in emissions, scavenging and optical properties of aerosols can have important impacts on the simulated AOD and subsequent forcing estimates within one model. Additional studies to place our estimates in the context of multi-model spread and provide a comprehensive uncertainty analysis are needed ahead of the IPCC Sixth Assessment Report.

Data availability

The CEDS anthropogenic emissions data is published within the ESGF system https://esgf-node.llnl.gov/search/input4mips/. Surface observations used in this study are collected from the following publicly available databases: the EBAS database (http://ebas.nilu.no/) hosted by NILU – Norwegian Institute for Air Research. The US national Clean Air Status and Trends monitoring network (CASTNET), available at http://www.epa.gov/castnet. The Interagency Monitoring of Protected Visual Environments (IMPROVE), a collaborative association of state, tribal, and federal agencies, and international partners, with the US EPA as the primary funding source and support from the National Park Service. Data available from http://vista.cira.colostate.edu/Improve/. MODIS and MISR AOD retrievals are downloaded from https://giovanni.gsfc.nasa.gov/giovanni/. Aircraft measurements from the HIPPO3 flights available from https://www.eol.ucar.edu/node/524. Model output available upon request from Marianne T. Lund (m.t.lund@cicero.oslo.no).

Code availability

The OsloCTM3 is stored in a SVN repository at the University of Oslo central subversion system and is available upon request. Please contact m.t.lund@cicero.oslo.no. In this paper, we use the official version 1.0, OsloCTM3v1.0.

supercomputing (NOTUR). The AeroCom database is maintained through basic funding from the Norwegian Meteorological Institute.

Competing interests
The authors declare that they have no conflict of interest.

References

Aiken, A. C., P. F. DeCarlo, J. H. Kroll, D. R. Worsnop, J. A. Huffman, K. S. Docherty, I. M. Ulbrich, C. Mohr, J. R. Kimmel, D. Sueper, Y. Sun, Q. Zhang, A. Trimborn, M. Northway, P. J. Ziemann, M. R. Canagaratna, T. B. Onasch, M. R. Alfarra, A. S. H. Prevot, J. Dommen, J. Duplissy, A. Metzger, U. Baltensperger, and J. L. Jimenez: O/C and OM/OC Ratios of Primary, Secondary, and Ambient Organic Aerosols with High-Resolution Time-of-Flight Aerosol Mass Spectrometry, Environmental Science & Technology, 42(12), 4478-4485, doi:10.1021/es703009q, **2008**

Amann, M., I. Bertok, J. Borken-Kleefeld, J. Cofala, C. Heyes, L. Höglund-Isaksson, Z. Klimont, B. Nguyen, M. Posch, P. Rafaj, R. Sandler, W. Schöpp, F. Wagner, and W. Winiwarter: Cost-effective control of air quality and greenhouse gases in Europe: Modeling and policy applications, Environmental Modelling & Software, 26(12), 1489-1501, doi:http://dx.doi.org/10.1016/j.envsoft.2011.07.012, **2011**

Berglen, T. F., T. K. Berntsen, I. S. A. Isaksen, and J. K. Sundet: A global model of the coupled sulfur/oxidant chemistry in the troposphere: The sulfur cycle, Journal of Geophysical Research-Atmospheres, 109(D19), doi:10.1029/2003jd003948, **2004**

Berntsen, T., J. Fuglestvedt, G. Myhre, F. Stordal, and T. F. Berglen: Abatement of greenhouse gases: Does location matter?, Climatic Change, 74(4), 377-411, doi:10.1007/s10584-006-0433-4, **2006**

Bian, H., M. Chin, D. A. Hauglustaine, M. Schulz, G. Myhre, S. E. Bauer, M. T. Lund, V. A. Karydis, T. L. Kucsera, X. Pan, A. Pozzer, R. B. Skeie, S. D. Steenrod, K. Sudo, K. Tsigaridis, A. P. Tsimpidi, and S. G. Tsyro: Investigation of global particulate nitrate from the AeroCom Phase III experiment, Atmos. Chem. Phys., 2017(17), 12911-12940, doi:https://doi.org/10.5194/acp-17-12911-2017, **2017**

Bond, T. C., and R. W. Bergstrom: Light absorption by carbonaceous particles: An investigative review, Aerosol Science and Technology, 40(1), 27-67, doi:10.1080/02786820500421521, **2006**

1040   Bond, T. C., S. J. Doherty, D. W. Fahey, P. M. Forster, T. Berntsen, B. J. DeAngelo, M. G. Flanner, S. Ghan,
1041   B. Kärcher, D. Koch, S. Kinne, Y. Kondo, P. K. Quinn, M. C. Sarofim, M. G. Schultz, M. Schulz, C.
1042   Venkataraman, H. Zhang, S. Zhang, N. Bellouin, S. K. Guttikunda, P. K. Hopke, M. Z. Jacobson, J. W.
1043   Kaiser, Z. Klimont, U. Lohmann, J. P. Schwarz, D. Shindell, T. Storelvmo, S. G. Warren, and C. S. Zender:
1044   Bounding the role of black carbon in the climate system: A scientific assessment, Journal of Geophysical
1045   Research: Atmospheres, 118(11), 5380-5552, doi:10.1002/jgrd.50171, **2013**

1046

1047   Boucher, O., D. Randall, P. Artaxo, C. Bretherton, G. Feingold, P. Forster, K. V.-M., Y. Kondo, H. Liao, U.
1048   Lohmann, P. Rasch, S. K. Satheesh, S. Sherwood, B. Stevens, and X. Y. Zhang Clouds and Aerosols: In:
1049   Climate Change 2013: The Physical Science Basis. Contribution of Working Group I to the Fifth
1050   Assessment Report of the Intergovernmental Panel on Climate Change [Stocker, T.F., D. Qin, G.-K.
1051   Plattner, M. Tignor, S.K. Allen, J. Boschung, A. Nauels, Y. Xia, V. Bex and P.M. Midgley (eds.)]. Cambridge
1052   University Press, Cambridge, United Kingdom and New York, NY, USA., **2013**

1053

1054   Bourgeois, Q., and I. Bey: Pollution transport efficiency toward the Arctic: Sensitivity to aerosol
1055   scavenging and source regions, Journal of Geophysical Research: Atmospheres, 116(D8), n/a-n/a,
1056   doi:10.1029/2010JD015096, **2011**

1057

1058   Browse, J., K. S. Carslaw, S. R. Arnold, K. Pringle, and O. Boucher: The scavenging processes controlling
1059   the seasonal cycle in Arctic sulphate and black carbon aerosol, Atmospheric Chemistry and Physics,
1060   12(15), 6775-6798, doi:10.5194/acp-12-6775-2012, **2012**

1061

1062   Carslaw, K. S., H. Gordon, D. S. Hamilton, J. S. Johnson, L. A. Regayre, M. Yoshioka, and K. J. Pringle:
1063   Aerosols in the Pre-industrial Atmosphere, Current Climate Change Reports, 3(1), 1-15,
1064   doi:10.1007/s40641-017-0061-2, **2017**

1065

1066   Cavalli, F., A. Alastuey, H. Areskoug, D. Ceburnis, J. Čech, J. Genberg, R. M. Harrison, J. L. Jaffrezo, G. Kiss,
1067   P. Laj, N. Mihalopoulos, N. Perez, P. Quincey, J. Schwarz, K. Sellegri, G. Spindler, E. Swietlicki, C.
1068   Theodosi, K. E. Yttri, W. Aas, and J. P. Putaud: A European aerosol phenomenology -4: Harmonized
1069   concentrations of carbonaceous aerosol at 10 regional background sites across Europe, Atmospheric
1070   Environment, 144, 133-145, doi:https://doi.org/10.1016/j.atmosenv.2016.07.050, **2016**

1071

1072   Cooke, W. F., C. Liousse, H. Cachier, and J. Feichter: Construction of a 1 degrees x 1 degrees fossil fuel
1073   emission data set for carbonaceous aerosol and implementation and radiative impact in the ECHAM4
1074   model, Journal of Geophysical Research-Atmospheres, 104(D18), 22137-22162,
1075   doi:10.1029/1999jd900187, **1999**

1076

1077   Dubovik, O., and M. D. King: A flexible inversion algorithm for retrieval of aerosol optical properties from
1078   Sun and sky radiance measurements, Journal of Geophysical Research: Atmospheres, 105(D16), 20673-
1079   20696, doi:10.1029/2000JD900282, **2000**

1080

1081   Eckhardt, S., B. Quennehen, D. J. L. Olivié, T. K. Berntsen, R. Cherian, J. H. Christensen, W. Collins, S.
1082   Crepinsek, N. Daskalakis, M. Flanner, A. Herber, C. Heyes, Ø. Hodnebrog, L. Huang, M. Kanakidou, Z.

1083 Klimont, J. Langner, K. S. Law, M. T. Lund, R. Mahmood, A. Massling, S. Myriokefalitakis, I. E. Nielsen, J. K.
1084 Nøjgaard, J. Quaas, P. K. Quinn, J. C. Raut, S. T. Rumbold, M. Schulz, S. Sharma, R. B. Skeie, H. Skov, T.
1085 Uttal, K. von Salzen, and A. Stohl: Current model capabilities for simulating black carbon and sulfate
1086 concentrations in the Arctic atmosphere: a multi-model evaluation using a comprehensive measurement
1087 data set, Atmos. Chem. Phys., 15(16), 9413-9433, doi:10.5194/acp-15-9413-2015, **2015**

1088

1089 Fan, S. M., J. P. Schwarz, J. Liu, D. W. Fahey, P. Ginoux, L. W. Horowitz, H. Levy, Y. Ming, and J. R.
1090 Spackman: Inferring ice formation processes from global-scale black carbon profiles observed in the
1091 remote atmosphere and model simulations, Journal of Geophysical Research: Atmospheres, 117(D23),
1092 D23205, doi:10.1029/2012JD018126, **2012**

1093

1094 Feng, Y., V. Ramanathan, and V. R. Kotamarthi: Brown carbon: a significant atmospheric absorber of
1095 solar radiation?, Atmos. Chem. Phys., 13(17), 8607-8621, doi:10.5194/acp-13-8607-2013, **2013**

1096

1097 Gantt, B., M. S. Johnson, M. Crippa, A. S. H. Prévôt, and N. Meskhidze: Implementing marine organic
1098 aerosols into the GEOS-Chem model, Geosci. Model Dev., 8(3), 619-629, doi:10.5194/gmd-8-619-2015,
1099 **2015**

1100

1101 Granier, C., B. Bessagnet, T. Bond, A. D'Angiola, H. Denier van der Gon, G. J. Frost, A. Heil, J. W. Kaiser, S.
1102 Kinne, Z. Klimont, S. Kloster, J.-F. Lamarque, C. Liousse, T. Masui, F. Meleux, A. Mieville, T. Ohara, J.-C.
1103 Raut, K. Riahi, M. G. Schultz, S. J. Smith, A. Thompson, J. van Aardenne, G. R. van der Werf, and D. P. van
1104 Vuuren: Evolution of anthropogenic and biomass burning emissions of air pollutants at global and
1105 regional scales during the 1980–2010 period, Climatic Change, 109(1), 163, doi:10.1007/s10584-011-
1106 0154-1, **2011**

1107

1108 Grini, A., G. Myhre, J. K. Sundet, and I. S. A. Isaksen: Modeling the annual cycle of sea salt in the global
1109 3D model Oslo CTM2: Concentrations, fluxes, and radiative impact, Journal of Climate, 15(13), 1717-
1110 1730, doi:10.1175/1520-0442(2002)015<1717:mtacos>2.0.co;2, **2002**

1111

1112 Grini, A., G. Myhre, C. S. Zender, and I. S. A. Isaksen: Model simulations of dust sources and transport in
1113 the global atmosphere: Effects of soil erodibility and wind speed variability, Journal of Geophysical
1114 Research-Atmospheres, 110(D2), doi:10.1029/2004jd005037, **2005**

1115

1116 Hodnebrog, Ø., G. Myhre, and B. H. Samset: How shorter black carbon lifetime alters its climate effect,
1117 Nat Commun, 5, 5065, doi:10.1038/ncomms6065, **2014**

1118

1119 Hoesly, R. M., S. J. Smith, L. Feng, Z. Klimont, G. Janssens-Maenhout, T. Pitkanen, J. J. Seibert, L. Vu, R. J.
1120 Andres, R. M. Bolt, T. C. Bond, L. Dawidowski, N. Kholod, J. I. Kurokawa, M. Li, L. Liu, Z. Lu, M. C. P.
1121 Moura, P. R. O'Rourke, and Q. Zhang: Historical (1750–2014) anthropogenic emissions of reactive gases
1122 and aerosols from the Community Emission Data System (CEDS), Geosci. Model Dev., 2018(11), 369-408,
1123 doi:https://doi.org/10.5194/gmd-11-369-2018, **2018**

1124

1125 Holben, B. N., T. F. Eck, I. Slutsker, D. Tanré, J. P. Buis, A. Setzer, E. Vermote, J. A. Reagan, Y. J. Kaufman,
1126 T. Nakajima, F. Lavenu, I. Jankowiak, and A. Smirnov: AERONET—A Federated Instrument Network and
1127 Data Archive for Aerosol Characterization, Remote Sensing of Environment, 66(1), 1-16,
1128 doi:https://doi.org/10.1016/S0034-4257(98)00031-5, **1998**

1129
1130 Hoyle, C. R., T. Berntsen, G. Myhre, and I. S. A. Isaksen: Secondary organic aerosol in the global aerosol-
1131 chemical transport model Oslo CTM2, Atmos. Chem. Phys., 7(5675-5694), **2007**

1132
1133 Jaeglé, L., P. K. Quinn, T. S. Bates, B. Alexander, and J. T. Lin: Global distribution of sea salt aerosols: new
1134 constraints from in situ and remote sensing observations, Atmos. Chem. Phys., 11(7), 3137-3157,
1135 doi:10.5194/acp-11-3137-2011, **2011**

1136
1137 Kinne, S., D. O'Donnell, P. Stier, S. Kloster, K. Zhang , H. Schmidt, S. Rast, M. Giorgetta, T. F. Eck, and B.
1138 Stevens: MAC-v1: A new global aerosol climatology for climate studies, J. Adv. Model. Earth Syst., 5, 704-
1139 740, doi:doi:10.1002/jame.20035, **2013**

1140
1141 Kipling, Z., P. Stier, C. E. Johnson, G. W. Mann, N. Bellouin, S. E. Bauer, T. Bergman, M. Chin, T. Diehl, S. J.
1142 Ghan, T. Iversen, A. Kirkevåg, H. Kokkola, X. Liu, G. Luo, T. van Noije, K. J. Pringle, K. von Salzen, M.
1143 Schulz, Ø. Seland, R. B. Skeie, T. Takemura, K. Tsigaridis, and K. Zhang: What controls the vertical
1144 distribution of aerosol? Relationships between process sensitivity in HadGEM3–UKCA and inter-model
1145 variation from AeroCom Phase II, Atmos. Chem. Phys., 16(4), 2221-2241, doi:10.5194/acp-16-2221-
1146 2016, **2016**

1147
1148 Kipling, Z., P. Stier, J. P. Schwarz, A. E. Perring, J. R. Spackman, G. W. Mann, C. E. Johnson, and P. J.
1149 Telford: Constraints on aerosol processes in climate models from vertically-resolved aircraft
1150 observations of black carbon, Atmos. Chem. Phys., 13(12), 5969-5986, doi:10.5194/acp-13-5969-2013,
1151 **2013**

1152
1153 Kirchstetter, T. W., T. Novakov, and P. V. Hobbs: Evidence that the spectral dependence of light
1154 absorption by aerosols is affected by organic carbon, Journal of Geophysical Research: Atmospheres,
1155 109(D21), n/a-n/a, doi:10.1029/2004JD004999, **2004**

1156
1157 Klimont, Z., K. Kupiainen, C. Heyes, P. Purohit, J. Cofala, P. Rafaj, J. Borken-Kleefeld, and W. Schöpp:
1158 Global anthropogenic emissions of particulate matter including black carbon, Atmos. Chem. Phys.,
1159 17(14), 8681-8723, doi:10.5194/acp-17-8681-2017, **2017**

1160
1161 Klimont, Z., S. J. Smith, and J. Cofala: The last decade of global anthropogenic sulfur dioxide: 2000–2011
1162 emissions, Environmental Research Letters, 8(1), 014003, **2013**

1163
1164 Kumar, R., M. C. Barth, G. G. Pfister, V. S. Nair, S. D. Ghude, and N. Ojha: What controls the seasonal
1165 cycle of black carbon aerosols in India?, Journal of Geophysical Research: Atmospheres, 120(15), 7788-
1166 7812, doi:10.1002/2015JD023298, **2015**

1167

1168 Lamarque, J. F., T. C. Bond, V. Eyring, C. Granier, A. Heil, Z. Klimont, D. Lee, C. Liousse, A. Mieville, B.
1169 Owen, M. G. Schultz, D. Shindell, S. J. Smith, E. Stehfest, J. Van Aardenne, O. R. Cooper, M. Kainuma, N.
1170 Mahowald, J. R. McConnell, V. Naik, K. Riahi, and D. P. van Vuuren: Historical (1850–2000) gridded
1171 anthropogenic and biomass burning emissions of reactive gases and aerosols: methodology and
1172 application, Atmos. Chem. Phys., 10(15), 7017-7039, doi:10.5194/acp-10-7017-2010, **2010**

1173

1174 Lavery, T. F., C. M. Rogers, R. Baumgardner, and K. P. Mishoe: Intercomparison of Clean Air Status and
1175 Trends Network Nitrate and Nitric Acid Measurements with Data from Other Monitoring Programs,
1176 Journal of the Air & Waste Management Association, 59(2), 214-226, doi:10.3155/1047-3289.59.2.214,
1177 **2009**

1178

1179 Lee, Y. H., J. F. Lamarque, M. G. Flanner, C. Jiao, D. T. Shindell, T. Berntsen, M. M. Bisiaux, J. Cao, W. J.
1180 Collins, M. Curran, R. Edwards, G. Faluvegi, S. Ghan, L. W. Horowitz, J. R. McConnell, J. Ming, G. Myhre,
1181 T. Nagashima, V. Naik, S. T. Rumbold, R. B. Skeie, K. Sudo, T. Takemura, F. Thevenon, B. Xu, and J. H.
1182 Yoon: Evaluation of preindustrial to present-day black carbon and its albedo forcing from Atmospheric
1183 Chemistry and Climate Model Intercomparison Project (ACCMIP), Atmospheric Chemistry and Physics,
1184 13(5), 2607-2634, doi:10.5194/acp-13-2607-2013, **2013**

1185

1186 Li, C., C. McLinden, V. Fioletov, N. Krotkov, S. Carn, J. Joiner, D. Streets, H. He, X. Ren, Z. Li, and R. R.
1187 Dickerson: India Is Overtaking China as the World's Largest Emitter of Anthropogenic Sulfur Dioxide,
1188 Scientific Reports, 7(1), 14304, doi:10.1038/s41598-017-14639-8, **2017**

1189

1190 Lund, M. T., and T. Berntsen: Parameterization of black carbon aging in the OsloCTM2 and implications
1191 for regional transport to the Arctic, Atmos. Chem. Phys., 12(15), 6999-7014, doi:10.5194/acp-12-6999-
1192 2012, **2012**

1193

1194 Lund, M. T., T. K. Berntsen, and B. H. Samset: Sensitivity of black carbon concentrations and climate
1195 impact to aging and scavenging in OsloCTM2–M7, Atmos. Chem. Phys., 17(9), 6003-6022,
1196 doi:10.5194/acp-17-6003-2017, **2017**

1197

1198 Lund, M. T., B. H. Samset, R. B. Skeie, D. Watson-Parris, J. M. Katich, J. P. Schwarz, and B. Weinzierl:
1199 Short Black Carbon lifetime inferred from a global set of aircraft observations. Accepted manuscript. ,
1200 npj Climate and Atmospheric Science 1, 31, doi:10.1038/s41612-018-0040-x, **2018**

1201

1202 Mahmood, R., K. von Salzen, M. Flanner, M. Sand, J. Langner, H. Wang, and L. Huang: Seasonality of
1203 global and Arctic black carbon processes in the Arctic Monitoring and Assessment Programme models,
1204 Journal of Geophysical Research: Atmospheres, 121(12), 7100-7116, doi:10.1002/2016JD024849, **2016**

1205

1206 McLinden, C. A., V. Fioletov, M. W. Shephard, N. Krotkov, C. Li, R. V. Martin, M. D. Moran, and J. Joiner:
1207 Space-based detection of missing sulfur dioxide sources of global air pollution, Nature Geoscience, 9,
1208 496, doi:10.1038/ngeo2724

1209   https://www.nature.com/articles/ngeo2724#supplementary-information, **2016**

1210
1211   Metzger, S., F. Dentener, M. Krol, A. Jeuken, and J. Lelieveld: Gas/aerosol partitioning - 2. Global
1212   modeling results, Journal of Geophysical Research-Atmospheres, 107(D16), doi:10.1029/2001jd001103,
1213   **2002a**

1214
1215   Metzger, S., F. Dentener, S. Pandis, and J. Lelieveld: Gas/aerosol partitioning: 1. A computationally
1216   efficient model, Journal of Geophysical Research-Atmospheres, 107(D16), doi:10.1029/2001jd001102,
1217   **2002b**

1218
1219   MISR (2018), Data product specification for the MISR level 2 aerosol product, Garay, M.J., et al.,
1220   https://eosweb.larc.nasa.gov/project/misr/DPS_AEROSOL_V023.20180125.pdf (accessed 04/26/2018),
1221   edited.
1222   MOD08: MODIS Level 3 Atmosphere Products (MOD 08), Data Products Handbook Volume 2.
1223   https://modis.gsfc.nasa.gov/data/dataprod/dataproducts.php?MOD_NUMBER=08 (accessed
1224   04/26/2018), **2018**

1225
1226   Myhre, G., W. Aas, R. Cherian, W. Collins, G. Faluvegi, M. Flanner, P. Forster, Ø. Hodnebrog, Z. Klimont,
1227   M. T. Lund, J. Mülmenstädt, C. Lund Myhre, D. Olivié, M. Prather, J. Quaas, B. H. Samset, J. L. Schnell, M.
1228   Schulz, D. Shindell, R. B. Skeie, T. Takemura, and S. Tsyro: Multi-model simulations of aerosol and ozone
1229   radiative forcing due to anthropogenic emission changes during the period 1990–2015, Atmos. Chem.
1230   Phys., 17(4), 2709-2720, doi:10.5194/acp-17-2709-2017, **2017**

1231
1232   Myhre, G., N. Bellouin, T. F. Berglen, T. K. Berntsen, O. Boucher, A. L. F. Grini, I. S. A. Isaksen, M.
1233   Johnsrud, M. I. Mishchenko, F. Stordal, and D. TanrÉ: Comparison of the radiative properties and direct
1234   radiative effect of aerosols from a global aerosol model and remote sensing data over ocean, Tellus B,
1235   59(1), 115-129, doi:10.1111/j.1600-0889.2006.00226.x, **2007**

1236
1237   Myhre, G., T. F. Berglen, M. Johnsrud, C. R. Hoyle, T. K. Berntsen, S. A. Christopher, D. W. Fahey, I. S. A.
1238   Isaksen, T. A. Jones, R. A. Kahn, N. Loeb, P. Quinn, L. Remer, J. P. Schwarz, and K. E. Yttri: Modelled
1239   radiative forcing of the direct aerosol effect with multi-observation evaluation, Atmospheric Chemistry
1240   and Physics, 9(4), 1365-1392, doi:10.5194/acp-9-1365-2009, **2009**

1241
1242   Myhre, G., A. Grini, and S. Metzger: Modelling of nitrate and ammonium-containing aerosols in presence
1243   of sea salt, Atmos. Chem. Phys., 6, 4809-4821, **2006**

1244
1245   Myhre, G., B. H. Samset, M. Schulz, Y. Balkanski, S. Bauer, T. K. Berntsen, H. Bian, N. Bellouin, M. Chin, T.
1246   Diehl, R. C. Easter, J. Feichter, S. J. Ghan, D. Hauglustaine, T. Iversen, S. Kinne, A. Kirkevåg, J. F.
1247   Lamarque, G. Lin, X. Liu, M. T. Lund, G. Luo, X. Ma, T. van Noije, J. E. Penner, P. J. Rasch, A. Ruiz, Ø.
1248   Seland, R. B. Skeie, P. Stier, T. Takemura, K. Tsigaridis, P. Wang, Z. Wang, L. Xu, H. Yu, F. Yu, J. H. Yoon, K.
1249   Zhang, H. Zhang, and C. Zhou: Radiative forcing of the direct aerosol effect from AeroCom Phase II
1250   simulations, Atmos. Chem. Phys., 13(4), 1853-1877, doi:10.5194/acp-13-1853-2013, **2013a**

1251

1252 Myhre, G., D. Shindell, F.-M. Brèon, W. Collins, J. Fuglestvedt, J. Huang, D. Koch, J.-F. Lamarque, D. Lee,
1253 B. Mendoza, T. Nakajima, A. Robock, G. Stephens, T. Takemura, and H. Zhang: Anthropogenic and
1254 natural radiative forcing. In: Climate Change 2013: The Physical Science Basis. Contribution of Working
1255 Group I to the Fifth Assessment Report of the Intergovernmental Panel on Climate Change [Stocker, T.F.,
1256 D., Qin, G.-K. Plattner, M. Tignor, S.K. Allen, J. Boschung, A. Nauels, Y. Xia, V. Bex and P.M. Midgley (eds).
1257 Cambridge University Press, Cambridge, United Kingdom and New York, NY, USA **2013b**

1258

1259 Neu, J. L., and M. J. Prather: Toward a more physical representation of precipitation scavenging in global
1260 chemistry models: cloud overlap and ice physics and their impact on tropospheric ozone, Atmos. Chem.
1261 Phys., 12(7), 3289-3310, doi:10.5194/acp-12-3289-2012, **2012**

1262

1263 Parhi, P., A. Giannini, P. Gentine, and U. Lall: Resolving Contrasting Regional Rainfall Responses to El
1264 Niño over Tropical Africa, Journal of Climate, 29(4), 1461-1476, doi:10.1175/jcli-d-15-0071.1, **2016**

1265

1266 Paul, G., P. J. M., G. T. E., H. N. Christina, and Z. Ming: Global‐scale attribution of anthropogenic and
1267 natural dust sources and their emission rates based on MODIS Deep Blue aerosol products, Reviews of
1268 Geophysics, 50(3), doi:doi:10.1029/2012RG000388, **2012**

1269

1270 Petzold, A., J. A. Ogren, M. Fiebig, P. Laj, S. M. Li, U. Baltensperger, T. Holzer-Popp, S. Kinne, G.
1271 Pappalardo, N. Sugimoto, C. Wehrli, A. Wiedensohler, and X. Y. Zhang: Recommendations for reporting
1272 "black carbon" measurements, Atmos. Chem. Phys., 13(16), 8365-8379, doi:10.5194/acp-13-8365-2013,
1273 **2013**

1274

1275 Putaud, J. P., R. Van Dingenen, A. Alastuey, H. Bauer, W. Birmili, J. Cyrys, H. Flentje, S. Fuzzi, R. Gehrig, H.
1276 C. Hansson, R. M. Harrison, H. Herrmann, R. Hitzenberger, C. Hüglin, A. M. Jones, A. Kasper-Giebl, G.
1277 Kiss, A. Kousa, T. A. J. Kuhlbusch, G. Löschau, W. Maenhaut, A. Molnar, T. Moreno, J. Pekkanen, C.
1278 Perrino, M. Pitz, H. Puxbaum, X. Querol, S. Rodriguez, I. Salma, J. Schwarz, J. Smolik, J. Schneider, G.
1279 Spindler, H. ten Brink, J. Tursic, M. Viana, A. Wiedensohler, and F. Raes: A European aerosol
1280 phenomenology – 3: Physical and chemical characteristics of particulate matter from 60 rural, urban,
1281 and kerbside sites across Europe, Atmospheric Environment, 44(10), 1308-1320,
1282 doi:https://doi.org/10.1016/j.atmosenv.2009.12.011, **2010**

1283

1284 Randerson, J. T., G. R. van der Werf, L. Giglio, G. J. Collatz, and P. S. Kasibhatla: Global Fire Emissions
1285 Database, Version 4.1 (GFEDv4). ORNL DAAC, Oak Ridge, Tennessee, USA. ,
1286 doi:https://doi.org/10.3334/ORNLDAAC/1293, **2017**

1287

1288 Sajeev, P., V. M. Randall, S. Graydon, L. W. Crystal, D. Aaron van, B. Michael, K. H. Daven, K. Zbigniew, V.
1289 Chandra, K. G. Sarath, and Z. Qiang: Anthropogenic fugitive, combustion and industrial dust is a
1290 significant, underrepresented fine particulate matter source in global atmospheric models,
1291 Environmental Research Letters, 12(4), 044018, **2017**

1292

1293 Samset, B. H., and G. Myhre: Climate response to externally mixed black carbon as a function of altitude,
1294 Journal of Geophysical Research: Atmospheres, 120(7), 2913-2927, doi:10.1002/2014JD022849, **2015**

1295
1296 Samset, B. H., G. Myhre, A. Herber, Y. Kondo, S. M. Li, N. Moteki, M. Koike, N. Oshima, J. P. Schwarz, Y.
1297 Balkanski, S. E. Bauer, N. Bellouin, T. K. Berntsen, H. Bian, M. Chin, T. Diehl, R. C. Easter, S. J. Ghan, T.
1298 Iversen, A. Kirkevåg, J. F. Lamarque, G. Lin, X. Liu, J. E. Penner, M. Schulz, Ø. Seland, R. B. Skeie, P. Stier,
1299 T. Takemura, K. Tsigaridis, and K. Zhang: Modelled black carbon radiative forcing and atmospheric
1300 lifetime in AeroCom Phase II constrained by aircraft observations, Atmos. Chem. Phys., 14(22), 12465-
1301 12477, doi:10.5194/acp-14-12465-2014, **2014**

1302
1303 Samset, B. H., G. Myhre, M. Schulz, Y. Balkanski, S. Bauer, T. K. Berntsen, H. Bian, N. Bellouin, T. Diehl, R.
1304 C. Easter, S. J. Ghan, T. Iversen, S. Kinne, A. Kirkevåg, J. F. Lamarque, G. Lin, X. Liu, J. E. Penner, Ø. Seland,
1305 R. B. Skeie, P. Stier, T. Takemura, K. Tsigaridis, and K. Zhang: Black carbon vertical profiles strongly affect
1306 its radiative forcing uncertainty, Atmos. Chem. Phys., 13(5), 2423-2434, doi:10.5194/acp-13-2423-2013,
1307 **2013**

1308
1309 Samset, B. H., C. W. Stjern, E. Andrews, R. A. Kahn, G. Myhre, M. Schulz, and G. L. Schuster: Aerosol
1310 Absorption: Progress Towards Global and Regional Constraints, Current Climate Change Reports,
1311 doi:10.1007/s40641-018-0091-4, **2018**

1312
1313 Sato, Y., H. Miura, H. Yashiro, D. Goto, T. Takemura, H. Tomita, and T. Nakajima: Unrealistically pristine
1314 air in the Arctic produced by current global scale models, Scientific Reports, 6, 26561,
1315 doi:10.1038/srep26561

1316 http://www.nature.com/articles/srep26561#supplementary-information, **2016**

1317
1318 Schutgens, N., S. Tsyro, E. Gryspeerdt, D. Goto, N. Weigum, M. Schulz, and P. Stier: On the spatio-
1319 temporal representativeness of observations, Atmos. Chem. Phys., 17(16), 9761-9780, doi:10.5194/acp-
1320 17-9761-2017, **2017**

1321
1322 Schutgens, N. A. J., E. Gryspeerdt, N. Weigum, S. Tsyro, D. Goto, M. Schulz, and P. Stier: Will a perfect
1323 model agree with perfect observations? The impact of spatial sampling, Atmos. Chem. Phys., 16(10),
1324 6335-6353, doi:10.5194/acp-16-6335-2016, **2016a**

1325
1326 Schutgens, N. A. J., D. G. Partridge, and P. Stier: The importance of temporal collocation for the
1327 evaluation of aerosol models with observations, Atmos. Chem. Phys., 16(2), 1065-1079,
1328 doi:10.5194/acp-16-1065-2016, **2016b**

1329
1330 Schwarz, J. P., B. H. Samset, A. E. Perring, J. R. Spackman, R. S. Gao, P. Stier, M. Schulz, F. L. Moore, E. A.
1331 Ray, and D. W. Fahey: Global-scale seasonally resolved black carbon vertical profiles over the Pacific,
1332 Geophysical Research Letters, 40(20), 2013GL057775, doi:10.1002/2013GL057775, **2013**

1333

1334   Sindelarova, K., C. Granier, I. Bouarar, A. Guenther, S. Tilmes, T. Stavrakou, J. F. Müller, U. Kuhn, P.
1335   Stefani, and W. Knorr: Global data set of biogenic VOC emissions calculated by the MEGAN model over
1336   the last 30 years, Atmos. Chem. Phys., 14(17), 9317-9341, doi:10.5194/acp-14-9317-2014, **2014**

1337

1338   Skeie, R. B., T. Berntsen, G. Myhre, C. A. Pedersen, J. Ström, S. Gerland, and J. A. Ogren: Black carbon in
1339   the atmosphere and snow, from pre-industrial times until present, Atmospheric Chemistry and Physics,
1340   11(14), 6809-6836, doi:10.5194/acp-11-6809-2011, **2011**

1341

1342   Smith, S. J., Y. Zhou, P. Kyle, H. Wang, and H. Yu: A Community Emissions Data System (CEDS): Emissions
1343   for CMIP6 and Beyond. , **2015**

1344

1345   Sofiev, M., J. Soares, M. Prank, G. de Leeuw, and J. Kukkonen: A regional-to-global model of emission
1346   and transport of sea salt particles in the atmosphere, Journal of Geophysical Research: Atmospheres,
1347   116(D21), n/a-n/a, doi:10.1029/2010JD014713, **2011**

1348

1349   Stamnes, K., S. C. Tsay, W. Wiscombe, and K. Jayaweera: Numerically stable algorithm for discrete-
1350   ordinate-method radiative transfer in multiple scattering and emitting layered media, Appl. Opt., 27(12),
1351   2502-2509, doi:10.1364/AO.27.002502, **1988**

1352

1353   Stjern, C. W., B. H. Samset, G. Myhre, P. M. Forster, Ø. Hodnebrog, T. Andrews, O. Boucher, G. Faluvegi,
1354   T. Iversen, M. Kasoar, V. Kharin, A. Kirkevåg, J.-F. Lamarque, D. Olivié, T. Richardson, D. Shawki, D.
1355   Shindell, C. J. Smith, T. Takemura, and A. Voulgarakis: Rapid Adjustments Cause Weak Surface
1356   Temperature Response to Increased Black Carbon Concentrations, Journal of Geophysical Research:
1357   Atmospheres, 122(21), 11,462-411,481, doi:10.1002/2017JD027326, **2017**

1358

1359   Søvde, O. A., M. J. Prather, I. S. A. Isaksen, T. K. Berntsen, F. Stordal, X. Zhu, C. D. Holmes, and J. Hsu: The
1360   chemical transport model Oslo CTM3, Geosci. Model Dev., 5(6), 1441-1469, doi:10.5194/gmd-5-1441-
1361   2012, **2012**

1362

1363   Taylor, K. E., R. J. Stouffer, and G. A. Meehl: An Overview of CMIP5 and the Experiment Design, Bulletin
1364   of the American Meteorological Society, 93(4), 485-498, doi:10.1175/bams-d-11-00094.1, **2012**

1365

1366   Thomson, A. M., K. V. Calvin, S. J. Smith, G. P. Kyle, A. Volke, P. Patel, S. Delgado-Arias, B. Bond-
1367   Lamberty, M. A. Wise, L. E. Clarke, and J. A. Edmonds: RCP4.5: a pathway for stabilization of radiative
1368   forcing by 2100, Climatic Change, 109(1), 77, doi:10.1007/s10584-011-0151-4, **2011**

1369

1370   Tsigaridis, K., N. Daskalakis, M. Kanakidou, P. J. Adams, P. Artaxo, R. Bahadur, Y. Balkanski, S. E. Bauer, N.
1371   Bellouin, A. Benedetti, T. Bergman, T. K. Berntsen, J. P. Beukes, H. Bian, K. S. Carslaw, M. Chin, G. Curci,
1372   T. Diehl, R. C. Easter, S. J. Ghan, S. L. Gong, A. Hodzic, C. R. Hoyle, T. Iversen, S. Jathar, J. L. Jimenez, J. W.
1373   Kaiser, A. Kirkevåg, D. Koch, H. Kokkola, Y. H. Lee, G. Lin, X. Liu, G. Luo, X. Ma, G. W. Mann, N.
1374   Mihalopoulos, J. J. Morcrette, J. F. Müller, G. Myhre, S. Myriokefalitakis, N. L. Ng, D. O'Donnell, J. E.
1375   Penner, L. Pozzoli, K. J. Pringle, L. M. Russell, M. Schulz, J. Sciare, Ø. Seland, D. T. Shindell, S. Sillman, R. B.

1376 Skeie, D. Spracklen, T. Stavrakou, S. D. Steenrod, T. Takemura, P. Tiitta, S. Tilmes, H. Tost, T. van Noije, P.
1377 G. van Zyl, K. von Salzen, F. Yu, Z. Wang, Z. Wang, R. A. Zaveri, H. Zhang, K. Zhang, Q. Zhang, and X.
1378 Zhang: The AeroCom evaluation and intercomparison of organic aerosol in global models, Atmos. Chem.
1379 Phys., 14(19), 10845-10895, doi:10.5194/acp-14-10845-2014, **2014**

1380

1381 Turpin, B. J., and H.-J. Lim: Species Contributions to PM2.5 Mass Concentrations: Revisiting Common
1382 Assumptions for Estimating Organic Mass, Aerosol Science and Technology, 35(1), 602-610,
1383 doi:10.1080/02786820119445, **2001**

1384

1385 Tørseth, K., W. Aas, K. Breivik, A. M. Fjæraa, M. Fiebig, A. G. Hjellbrekke, C. Lund Myhre, S. Solberg, and
1386 K. E. Yttri: Introduction to the European Monitoring and Evaluation Programme (EMEP) and observed
1387 atmospheric composition change during 1972 - 2009, Atmos. Chem. Phys., 12(12), 5447-5481,
1388 doi:10.5194/acp-12-5447-2012, **2012**

1389

1390 van Marle, M. J. E., S. Kloster, B. I. Magi, J. R. Marlon, A. L. Daniau, R. D. Field, A. Arneth, M. Forrest, S.
1391 Hantson, N. M. Kehrwald, W. Knorr, G. Lasslop, F. Li, S. Mangeon, C. Yue, J. W. Kaiser, and G. R. van der
1392 Werf: Historic global biomass burning emissions for CMIP6 (BB4CMIP) based on merging satellite
1393 observations with proxies and fire models (1750–2015), Geosci. Model Dev., 10(9), 3329-3357,
1394 doi:10.5194/gmd-10-3329-2017, **2017**

1395

1396 van Vuuren, D. P., J. Edmonds, M. Kainuma, K. Riahi, A. Thomson, K. Hibbard, G. C. Hurtt, T. Kram, V.
1397 Krey, J.-F. Lamarque, T. Masui, M. Meinshausen, N. Nakicenovic, S. J. Smith, and S. K. Rose: The
1398 representative concentration pathways: an overview, Climatic Change, 109(1), 5, doi:10.1007/s10584-
1399 011-0148-z, **2011**

1400

1401 Wang, R., E. Andrews, Y. Balkanski, O. Boucher, G. Myhre, B. H. Samset, M. Schulz, G. L. Schuster, M.
1402 Valari, and S. Tao: Spatial Representativeness Error in the Ground-Level Observation Networks for Black
1403 Carbon Radiation Absorption, Geophysical Research Letters, 45, 2106-2114,
1404 doi:10.1002/2017GL076817, **2018**

1405

1406 Wang, R., Y. Balkanski, O. Boucher, P. Ciais, G. L. Schuster, F. Chevallier, B. H. Samset, J. Liu, S. Piao, M.
1407 Valari, and S. Tao: Estimation of global black carbon direct radiative forcing and its uncertainty
1408 constrained by observations, Journal of Geophysical Research: Atmospheres, 121(10), 5948-5971,
1409 doi:10.1002/2015JD024326, **2016**

1410

1411 Wang, R., S. Tao, Y. Balkanski, P. Ciais, O. Boucher, J. Liu, S. Piao, H. Shen, M. R. Vuolo, M. Valari, H.
1412 Chen, Y. Chen, A. Cozic, Y. Huang, B. Li, W. Li, G. Shen, B. Wang, and Y. Zhang: Exposure to ambient black
1413 carbon derived from a unique inventory and high-resolution model, Proceedings of the National
1414 Academy of Sciences, 111(7), 2459-2463, doi:10.1073/pnas.1318763111, **2014**

1415

1416 Witek, M. L., D. J. Diner, and M. J. Garay: Satellite assessment of sea spray aerosol productivity:
1417 Southern Ocean case study, Journal of Geophysical Research: Atmospheres, 121(2), 872-894,
1418 doi:10.1002/2015JD023726, **2016**

1419
1420 Wofsy, S. C., H. S. Team, T. Cooperating Modellers, and T. Satellite: HIAPER Pole-to-Pole Observations
1421 (HIPPO): fine-grained, global-scale measurements of climatically important atmospheric gases and
1422 aerosols, Philosophical Transactions of the Royal Society a-Mathematical Physical and Engineering
1423 Sciences, 369(1943), 2073-2086, doi:10.1098/rsta.2010.0313, **2011**

1424
1425 Xie, M., M. D. Hays, and A. L. Holder: Light-absorbing organic carbon from prescribed and laboratory
1426 biomass burning and gasoline vehicle emissions, Scientific Reports, 7(1), 7318, doi:10.1038/s41598-017-
1427 06981-8, **2017**

1428
1429 Zanatta, M., M. Gysel, N. Bukowiecki, T. Müller, E. Weingartner, H. Areskoug, M. Fiebig, K. E. Yttri, N.
1430 Mihalopoulos, G. Kouvarakis, D. Beddows, R. M. Harrison, F. Cavalli, J. P. Putaud, G. Spindler, A.
1431 Wiedensohler, A. Alastuey, M. Pandolfi, K. Sellegri, E. Swietlicki, J. L. Jaffrezo, U. Baltensperger, and P.
1432 Laj: A European aerosol phenomenology-5: Climatology of black carbon optical properties at 9 regional
1433 background sites across Europe, Atmospheric Environment, 145, 346-364,
1434 doi:https://doi.org/10.1016/j.atmosenv.2016.09.035, **2016**

1435
1436 Zender, C. S., H. Bian, and D. Newman: Mineral Dust Entrainment and Deposition (DEAD) model:
1437 Description and 1990s dust climatology, Journal of Geophysical Research: Atmospheres, 108(D14),
1438 doi:doi:10.1029/2002JD002775, **2003**

1439
1440 Zhang, X. Y., Y. Q. Wang, T. Niu, X. C. Zhang, S. L. Gong, Y. M. Zhang , and J. Y. Sun: Atmospheric aerosol
1441 compositions in China: spatial/temporal variability, chemical signature, regional haze distribution and
1442 comparison with global models. , Atmos. Chem. Phys., 12, 779-799, **2012**

1443
1444
1445
1446
1447
1448
1449
1450
1451
1452
1453
1454
1455
1456
1457
1458
1459

1460
1461
1462
1463
1464
1465
1466
1467
1468
1469
1470
1471
1472
1473
1474

1475 Tables

1476

1477 *Table 1: Summary and description of simulations in this study*

Name	Athropogenic emissions	Year	Res	Description
CEDSv16/CMIP6	CEDS, version released in 2016	2010	2x2	Baseline simulation, 2.25x2.25 degree resolution
ECLv5	ECLIPSEv5	2010	2x2	As baseline, but with ECLIPSEv5 emissions
RCP/CMIP5	RCP4.5	2010	2x2	As baseline, but RCP4.5/CMIP5 emissions
LSIDEC	CEDS	2010	2x2	Reduced scavenging of all aerosols by large-scale ice clouds
LSIINC	CEDS	2010	2x2	Increased scavenging of all aerosols by large-scale ice clouds
SOLDEC	CEDS	2010	2x2	Decreased scavenging of all aerosols by convective and large-scale liquid preciptation
1x1RES	CEDS	2010	1x1	Same as baseline, but on 1.125x1.125 degree resolution
METDTA	CEDS	2010	2x2	Year 2010 emissions, but 2000 meteorology
Historical	CEDS/	1750-2014	2x2	Time-slice simulations for year 1750, 1850, 1900, 1910, 1920, 1930, 1940, 1950, 1960, 1970, 1980, 1985, 1990, 1995, 2000, 2005, 2010, 2014

1483 *Table 2: Fraction of aerosol mass available for wet scavenging by convective, large-scale liquid*

1484 *and large-scale ice precipitation in baseline setup and in the three sensitivity tests.*

1485 *Phil=hydrophilic, phob=hydrophobic.*

Simulation	Precipitation type	Sulfate	OM phil	OM phob	BC phil	BC Phob	Nitrate	SOA	Sea salt	Dust
CEDSv16/ CMIP6	Convective	1	1	1	1	1	1	0.8	1	1
	LS-liquid	1	1	0	1	0	1	0.8	1	1
	LS-ice	0.1	0.1	0.2	0.1	0.2	0.1	0.16	0.1	0.5
LSIINC	LS-ice	0.3	0.3	0.4	0.3	0.4	0.3	0.32	0.3	0.7
LSIDEC	LS-ice	0.001	0.001	0.1	0.001	0.1	0.001	0.001	0.001	0.1
SOLDEC	Convective	0.8	0.8	0.8	0.8	0.8	0.8	0.6	0.8	0.8
	LS-liquid	0.8	0.8	0	0.8	0	0.8	0.6	0.8	0.8

1487

1488

1489

1490

Table 3: Global, annual mean aerosol burdens [mg m^{-2}] and total AOD in the baseline and sensitivity simulations. Parentheses in the top row give~~show~~ the atmospheric residence time (ratio of burden to total wet plus dry scavenging) [days]. Corresponding values for the sensitivity simulations are given in Table S3. ~~ratio of the sensitivity test to the baseline CEDSv16/CMIP6.~~

Simulation	BC	OA	Sulfate	NH4 (fine+coarse)	Nitrate (fine)	Nitrate (coarse)	Sea salt	Dust	AOD
CEDS/CMIP6	**0.23** **(4.4)**	**3.4**[§] **(5.3)**	**5.4** **(5.4)**	**0.68** **(3.5)**	**0.17** **(4.2)**	**3.9** **(5.2)**	**12** **(0.46)**	**39** **(3.4)**	**0.13**
ECLv5	0.21	3.1	5.1	0.65	0.15	3.7	12	39	0.13
RCP/CMIP5	0.18	3.2	5.3	0.63	0.13	3.7	12	39	0.13
LSIINC	0.21	2.8	4.9	0.63	0.17	3.4	11	39	0.12
LSIDEC	0.32	5.3	6.5	0.79	0.16	4.7	14	43	0.16
SOLDEC	0.26	3.6	6.1	0.78	0.16	5.2	15	42	0.15
1x1RES	0.24	3.4	5.6	0.71	0.19	3.6	12	38	0.14
METDTA	0.22	3.0	5.5	0.69	0.16	3.8	12	42	0.13

[§] SOA: 1.1 mg m^{-2} [5.8 days] and POA: 2.3 mg m^{-2} [5.1 days]

1508
1509
1510
1511
1512
1513
1514
1515
1516
1517
1518
1519
1520
1521
1522
1523
1524
1525
1526
1527
1528
1529
1530
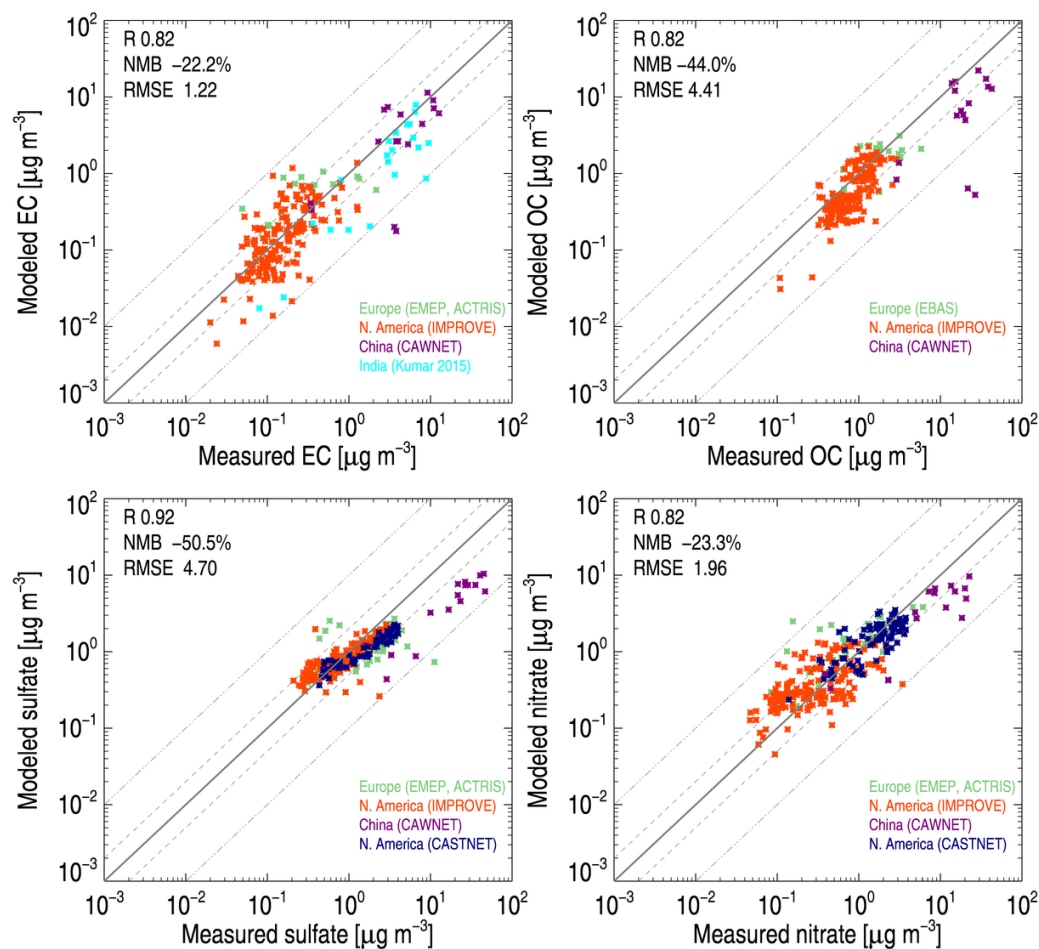1531
1532
1533
1534
1535
1536
1537   Figures

1538

1539

1540 *Figure 1: Annual mean modeled versus measured aerosol surface concentrations of a) EC, b)*
1541 *OC, c) sulfate and d) nitrate from the IMPROVE, EMEP, ACTRIS, CASTNET and CAWNET*
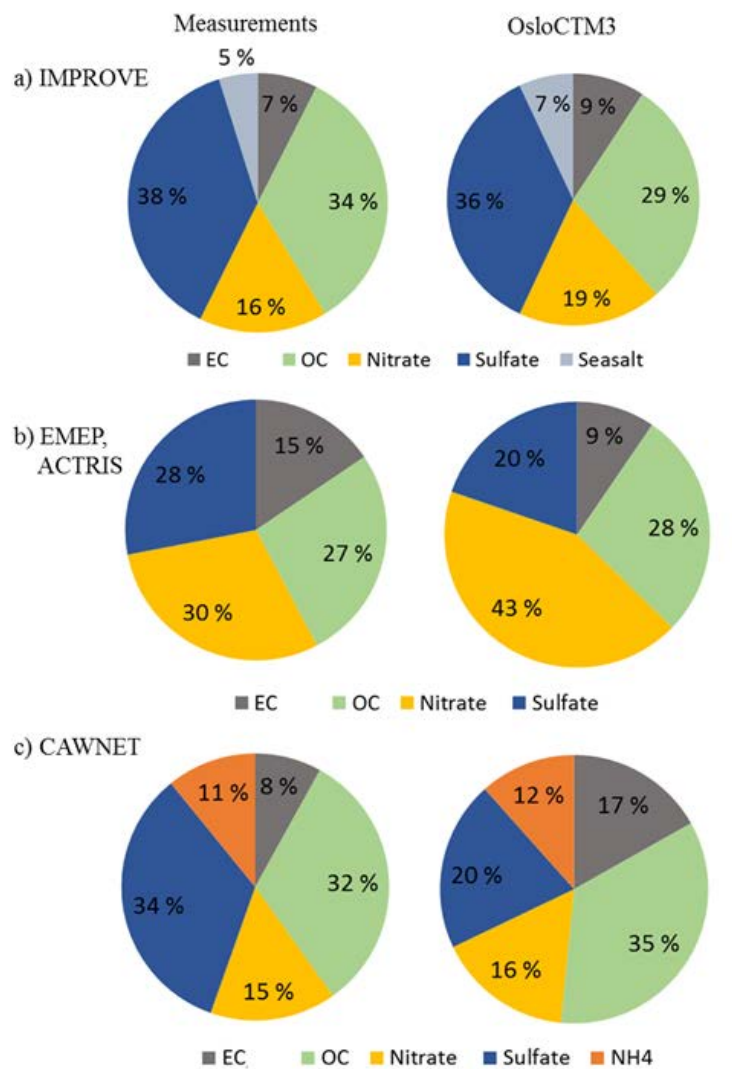1542 *measurements networks.*

1543

1544

Figure 2: Aerosol composition (fraction of total aerosol mass) derived from the IMPROVE, EMEP, ACTRIS and CAWNET networks (left column) and corresponding OsloCTM3 results (right column).

1548

1549

1550
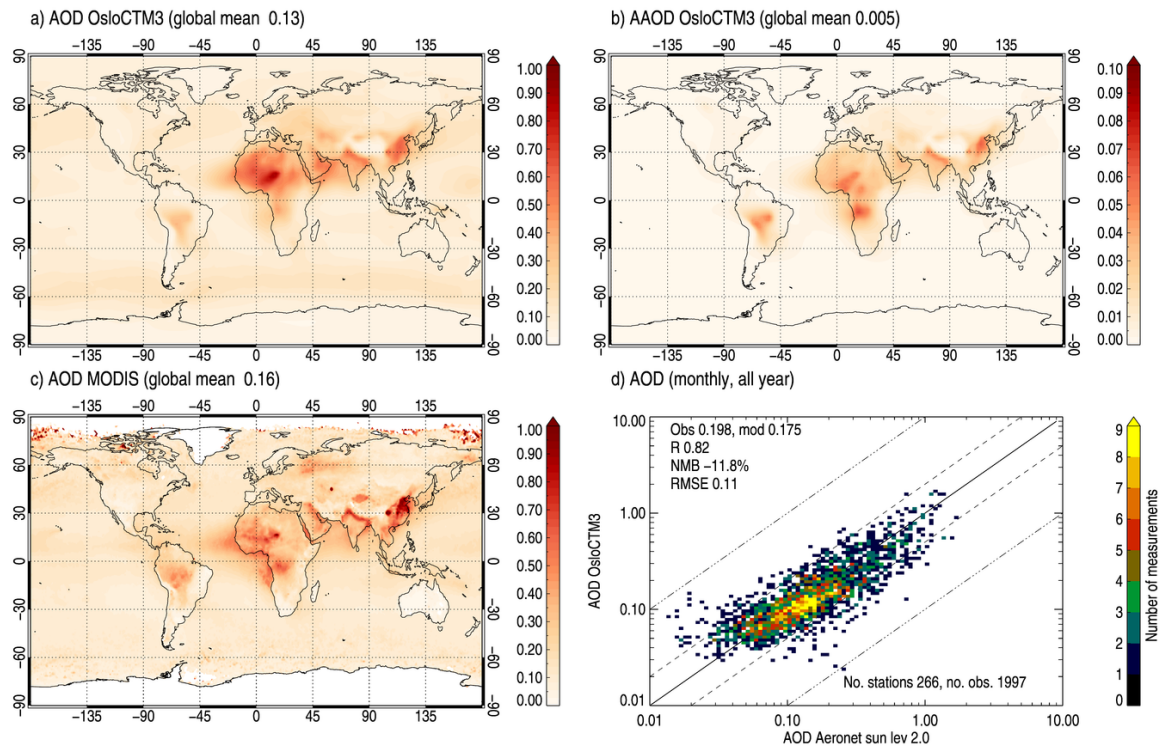
Figure 3: Annual mean (year 2010) modeled a) AOD and b) AAOD, c) MODIS-Aqua AOD retrieval and d) scatter density plot of comparison of simulated AOD against monthly mean AERONET observations.

1551
1552
1553

1554

1555

1556

1557
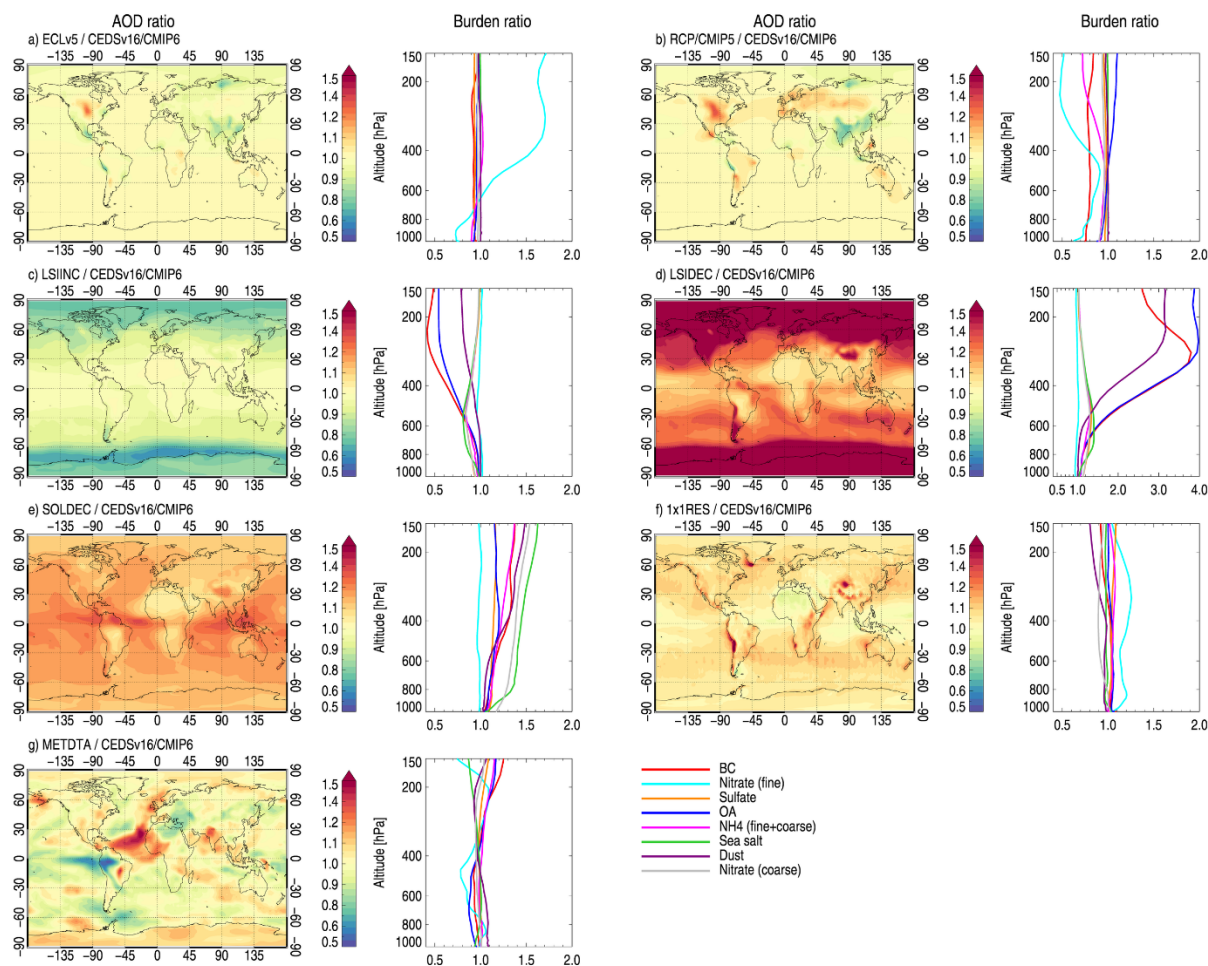
Figure 4: Ratio of each sensitivity simulation relative to the baseline for AOD (columns 1 and 3)
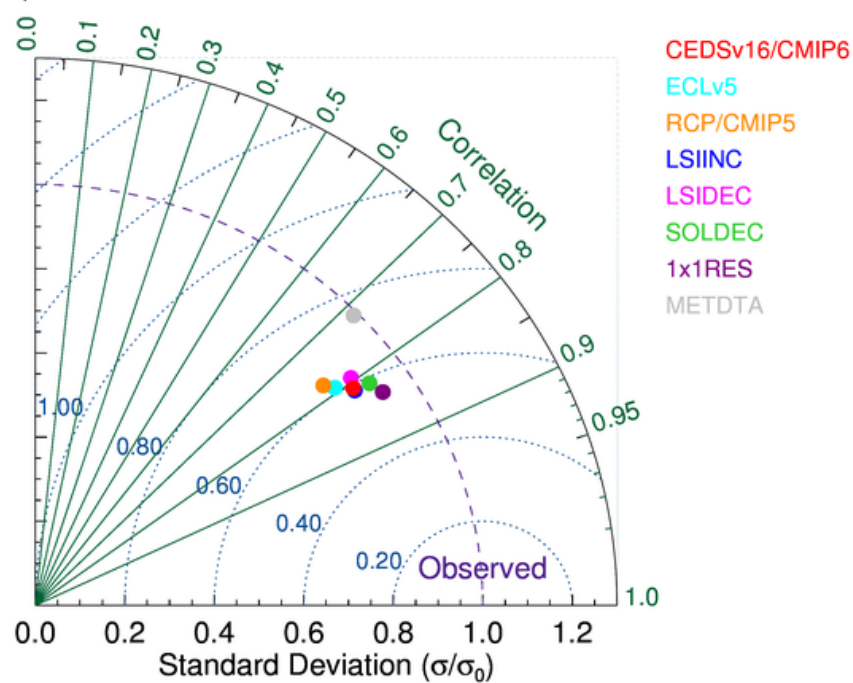*and total burden by species in each model layer (columns 2 and 4).*

1558

1559

1560

1561

a) Surface concentration

1562

b) AOD

1563
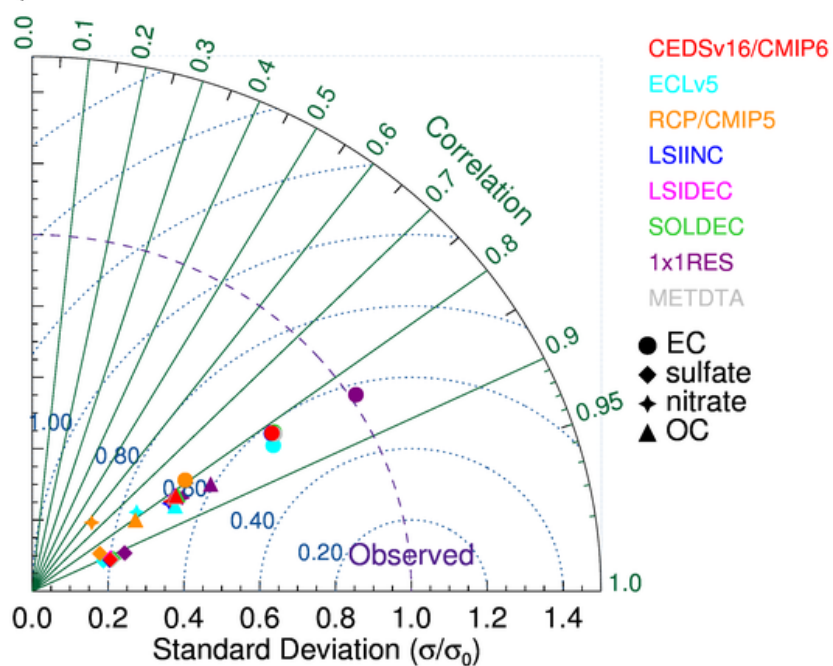
Figure 5: Taylor diagram of modeled and measured aerosol surface concentrations in the baseline simulation and sensitivity tests using all observations in Fig. 1.
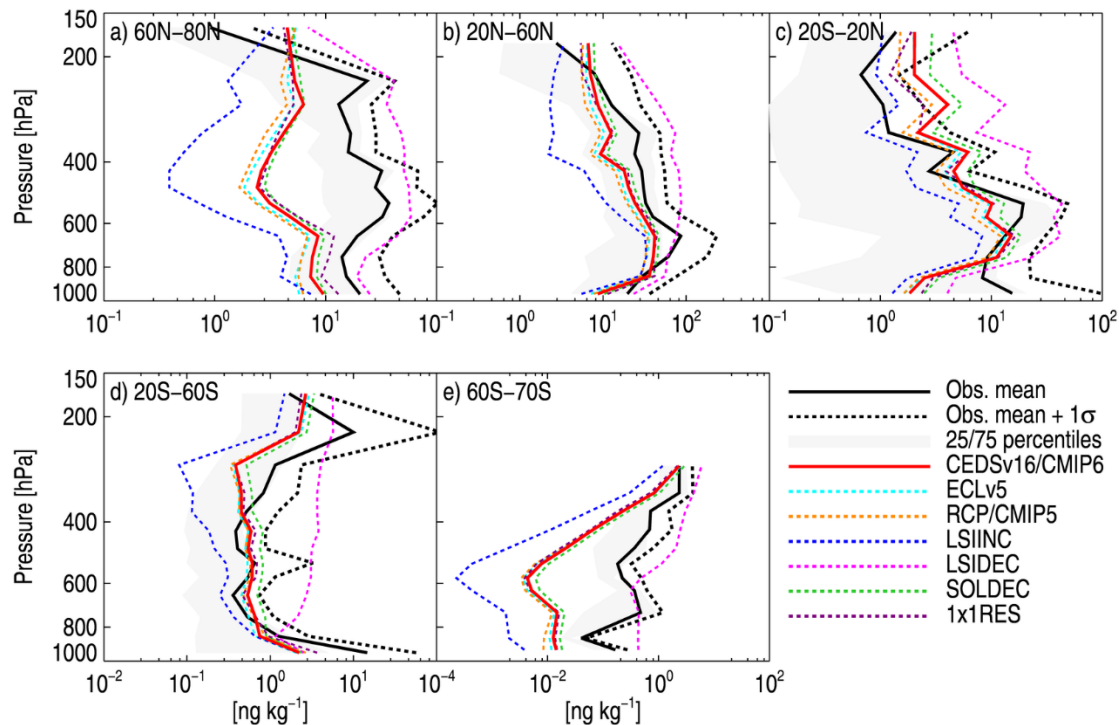
1564
1565

1566
1567

Figure 6: Modeled vertical BC profiles against rBC aircraft measurements in five different latitudes bands over the Pacific Ocean from the HIPPO3 flight campaign. Model data is extracted along the flight track using an online flight simulator. Black lines: mean of observations (solid), mean + plus 1 standard deviation (dashed). Colored lines: OsloCTM3 baseline (CEDSv16/CMIP6) (solid), sensitivity simulations (dashed).
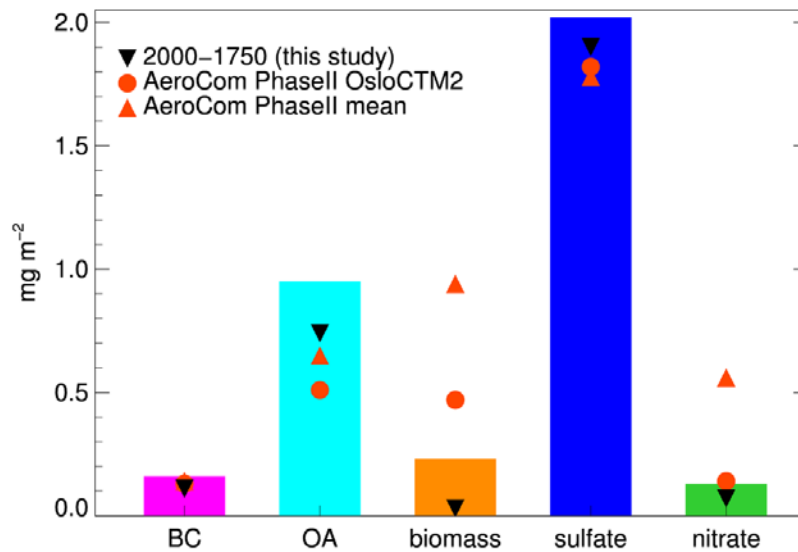
1582

Figure 7: Change in anthropogenic aerosol load over the period 1750 to 2014 using CEDSv16
emissions. Black symbols show the 1750 to 2000 difference and red symbols show multi-model
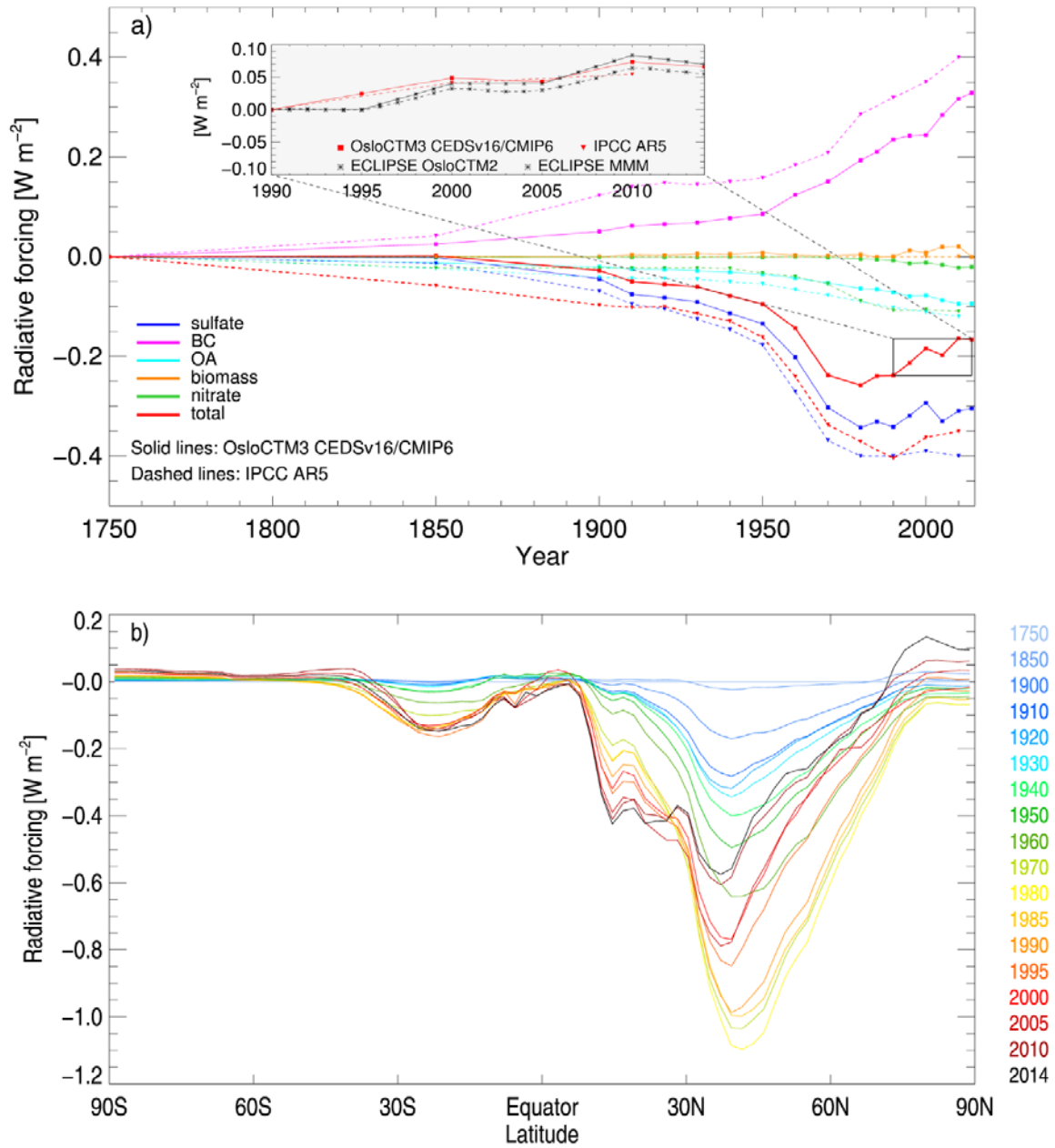*mean and OsloCTM2 results from the AeroCom II experiments [Myhre et al., 2013a].*

1583

1584

1585

1586

1587

1588

1589

1590

Figure 8: a) Time evolution of RFari. Solid lines show OsloCTM3 results from the current study, while dashed lines show results from IPCC AR5[Myhre et al., 2013b]. The inset shows the change in total RFari between 1990 and 2015 in the current study compared with IPCC AR5 and multi-model mean and OsloCTM2 results from Myhre et al. [2017] using ECLv5 emissions. b) zonal mean RFari 1750-2014.

1596